Disclosure statement

The authors declare no competing interests.

References

1. Tantillo C, Ding J, Jacobo-Molina A, *et al.* Locations of anti-AIDS drug binding sites and resistance mutations in the three-dimensional structure of HIV-1 reverse transcriptase. Implications for mechanisms of drug inhibition and resistance. *J Mol Biol* 1994; **243**:369–387.
2. Mitchla Z, Sharland M. Current treatment options to prevent perinatal transmission of HIV. *Expert Opin Pharmacother* 2000; **1**:239–248.
3. Lallemant M, Jourdain G, Le Coeur S, *et al.* Single-dose perinatal nevirapine plus standard zidovudine to prevent mother-to-child transmission of HIV-1 in Thailand. *N Engl J Med* 2004; **351**:217–228.
4. Adkins JC, Noble S. Efavirenz. *Drugs* 1998; **56**:1055–1064.
5. Staszewski S, Morales-Ramirez J, Tashima KT, *et al.* Efavirenz plus zidovudine and lamivudine, efavirenz plus indinavir, and indinavir plus zidovudine and lamivudine in the treatment of HIV-1 infection in adults. Study 006 Team. *N Engl J Med* 1999; **341**:1865–1873.
6. Lucas GM, Chaisson RE, Moore RD. Comparison of initial combination antiretroviral therapy with a single protease inhibitor, ritonavir and saquinavir, or efavirenz. *AIDS* 2001; **15**:1679–1686.
7. Robbins GK, De Gruttola V, Shafer RW, *et al.* Comparison of sequential three-drug regimens as initial therapy for HIV-1 infection. *N Engl J Med* 2003; **349**:2293–2303.
8. Gulick RM, Ribaudo HJ, Shikuma CM, *et al.* Triple-nucleoside regimens versus efavirenz-containing regimens for the initial treatment of HIV-1 infection. *N Engl J Med* 2004; **350**:1850–1861.
9. Hsiou Y, Ding J, Das K, *et al.* The Lys103Asn mutation of HIV-1 RT: a novel mechanism of drug resistance. *J Mol Biol* 2001; **309**:437–445.
10. Richman DD, ACTG 164/168 Study Team. Loss of nevirapine activity associated with emergence of resistance in clinical trials. *VIII International Conference on AIDS/ III STD World Congress*. 19–24 July 1992, Amsterdam, the Netherlands. Abstract PoB 3576.
11. Richman DD, Shih C-K, Lowy I, *et al.* Human immunodeficiency virus type 1 mutants resistant to nonnucleoside inhibitors of reverse transcriptase arise in tissue culture. *Proc Natl Acad Sci U S A* 1991; **88**:11241–11245.
12. Bacheler L, Jeffrey S, Hanna G, *et al.* Genotypic correlates of phenotypic resistance to efavirenz in virus isolates from patients failing nonnucleoside reverse transcriptase inhibitor therapy. *J Virol* 2001; **75**:4999–5008.
13. Bacheler LT, Anton ED, Kudish P, *et al.* Human immunodeficiency virus type 1 mutations selected in patients failing efavirenz combination therapy. *Antimicrob Agents Chemother* 2000; **44**:2475–2484.
14. Masuda N, Yamamoto O, Fujii M, *et al.* Studies of non-nucleoside HIV-1 reverse transcriptase inhibitors. Part 2: Synthesis and structure-activity relationships of 2-cyano and 2-hydroxy thiazolidenebenzenesulfonamide derivatives. *Bioorg Med Chem* 2005; **13**:949–961.
15. Fujiwara M, Ijichi K, Hanasaki Y, *et al.* Thiadiazole derivatives: highly potent and selective inhibitors of human immunodeficiency virus type 1 (HIV-1) replications *in vitro*. *Microbiol Immunol* 1997; **41**:301–308.
16. Fujiwara M, Kodama EN, Okamoto M, *et al.* Characterization of human immunodeficiency virus type 1 strains resistant to the non-nucleoside reverse transcriptase inhibitor RD4-2217. *Antivir Chem Chemother* 1999; **10**:315–320.
17. Masuda N, Yamamoto O, Fujii M, *et al.* Studies of nonnucleoside HIV-1 reverse transcriptase inhibitors. Part 1: design and synthesis of thiazolidenebenzenesulfonamides. *Bioorg Med Chem* 2004; **12**:6171–6182.
18. Kimpton J, Emerman M. Detection of replication-competent and pseudotyped human immunodeficiency virus with a sensitive cell line on the basis of activation of an integrated beta-galactosidase gene. *J Virol* 1992; **66**:2232–2239.
19. Kodama EI, Kohgo S, Kitano K, *et al.* 4'-Ethynyl nucleoside analogs: potent inhibitors of multidrug-resistant human immunodeficiency virus variants *in vitro*. *Antimicrob Agents Chemother* 2001; **45**:1539–1546.
20. Nameki D, Kodama E, Ikeuchi M, *et al.* Mutations conferring resistance to human immunodeficiency virus type 1 fusion inhibitors are restricted by gp41 and Rev-responsive element functions. *J Virol* 2005; **79**:764–770.
21. Shimura K, Kodama E, Sakagami Y, *et al.* Broad antiretroviral activity and resistance profile of the novel human immunodeficiency virus integrase inhibitor elvitegravir (JTK-303/GS-9137). *J Virol* 2008; **82**:764–774.
22. Jones G, Willett P, Glen RC. Molecular recognition of receptor sites using a genetic algorithm with a description of desolvation. *J Mol Biol* 1995; **245**:43–53.
23. Berman HM, Westbrook J, Feng Z, *et al.* The Protein Data Bank. *Nucleic Acids Res* 2000; **28**:235–242.
24. Protein data base, NCBI Structure. (Accessed 27 May 2008.) Available from http://www.ncbi.nlm.nih.gov/Structure/
25. Ren J, Milton J, Weaver KL, Short SA, Stuart DI, Stammers DK. Structural basis for the resilience of efavirenz (DMP-266) to drug resistance mutations in HIV-1 reverse transcriptase. *Structure Fold Des* 2000; **8**:1089–1094.
26. Allen FH. The Cambridge Structural Database: a quarter of a million crystal structures and rising. *Acta Crystallogr* B 2002; **58**:380–388.
27. Kantor R, Machekano R, Gonzales MJ, Dupnik K, Schapiro JM, Shafer RW. Human Immunodeficiency Virus Reverse Transcriptase and Protease Sequence Database: an expanded data model integrating natural language text and sequence analysis programs. *Nucleic Acids Res* 2001; **29**:296–299.
28. Shafer RW. Stanford HIV Drug Resistance Database, NNRTI Resistance notes. (Accessed 27 May 2008.) Available from http://hivdb.stanford.edu/cgi-bin/ NNRTIResiNote.cgi 2008
29. Clark SA, Calef C, Mellors JW. Mutations in retroviral genes associated with drug resistance. In *HIV Sequence Compendium 2005*. Edited by T Leitner, B Hahn, P Marx, F McCutchan, J Mellors, S Wolinsky & B Korber. New Mexico: Los Alamos National Laboratory 2005; pp. 80–174.
30. Parikh U, Calef C, Clark SA, Mellors JW. Mutations in retroviral genes associated with drug resistance. In *HIV Sequence Compendium 2003*. Edited by T Leitner, B Hahn, P Marx, F McCutchan, J Mellors, S Wolinsky & B Korber. New Mexico: Los Alamos National Laboratory 2003; pp. 38–122.
31. Balzarini J, Kleim JP, Riess G, Camarasa MJ, De Clercq E, Karlsson A. Sensitivity of (138 Glu->Lys) mutated human immunodeficiency virus type 1 (HIV-1) reverse transcriptase (RT) to HIV-1-specific RT inhibitors. *Biochem Biophys Res Commun* 1994; **201**:1305–1312.
32. Schinazi RF, Larder BA, Mellors JW. Mutations in retroviral genes associated with drug resistance: 1999–2000 update. *Int Antiviral News* 1999; **7**:46–69.
33. Ding J, Das K, Moereels H, *et al.* Structure of HIV-1 RT/ TIBO R 86183 complex reveals similarity in the binding of diverse nonnucleoside inhibitors. *Nat Struct Biol* 1995; **2**:407–415.
34. Ren J, Esnouf R, Garman E, *et al.* High resolution structures of HIV-1 RT from four RT-inhibitor complexes. *Nat Struct Biol* 1995; **2**:293–302.
35. Smerdon SJ, Jager J, Wang J, *et al.* Structure of the binding site for nonnucleoside inhibitors of the reverse transcriptase of human immunodeficiency virus type 1. *Proc Natl Acad Sci U S A* 1994; **91**:3911–3915.
36. Kohlstaedt LA, Wang J, Friedman JM, Rice PA, Steitz TA. Crystal structure at 3.5 A resolution of HIV-1 reverse transcriptase complexed with an inhibitor. *Science* 1992; **256**:1783–1790.

37. Esnouf R, Ren J, Ross C, Jones Y, Stammers D, Stuart D. Mechanism of inhibition of HIV-1 reverse transcriptase by non-nucleoside inhibitors. *Nat Struct Biol* 1995; **2**:303–308.

38. Spence RA, Kati WM, Anderson KS, Johnson KA. Mechanism of inhibition of HIV-1 reverse transcriptase by nonnucleoside inhibitors. *Science* 1995; **267**:988–993.

39. Das K, Lewi PJ, Hughes SH, Arnold E. Crystallography and the design of anti-AIDS drugs: conformational flexibility and positional adaptability are important in the design of non-nucleoside HIV-1 reverse transcriptase inhibitors. *Prog Biophys Mol Biol* 2005; **88**:209–231.

40. Das K, Clark AD, Jr, Lewi PJ, *et al.* Roles of conformational and positional adaptability in structure-based design of TMC125-R165335 (etravirine) and related non-nucleoside reverse transcriptase inhibitors that are highly potent and effective against wild-type and drug-resistant HIV-1 variants. *J Med Chem* 2004; **47**:2550–2560.

41. Palmer S, Margot N, Gilbert H, Shaw N, Buckheit R, Jr, Miller M. Tenofovir, adefovir, and zidovudine susceptibilities of primary human immunodeficiency virus type 1 isolates with non-B-subtypes or nucleoside resistance. *AIDS Res Hum Retroviruses* 2001; **17**:1167–1173.

42. Srinivas RV, Fridland A. Antiviral activities of 9-*R*-2-phosphonomethoxypropyl adenine (PMPA) and bis(isopropyloxymethylcarbonyl)PMPA against various drug-resistant human immunodeficiency virus strains. *Antimicrob Agents Chemother* 1998; **42**:1484–1487.

43. Tuske S, Sarafianos SG, Clark AD, Jr, *et al.* Structures of HIV-1 RT-DNA complexes before and after incorporation of the anti-AIDS drug tenofovir. *Nat Struct Mol Biol* 2004; **11**:469–474.

44. Yoshimura K, Kato R, Yusa K, *et al.* JE-2147: a dipeptide protease inhibitor (PI) that potently inhibits multi-PI-resistant HIV-1. *Proc Natl Acad Sci U S A* 1999; **96**:8675–8680.

Received 30 May 2008, accepted 10 July 2008

Antiviral Research 80 (2008) 71–76

Contents lists available at ScienceDirect

Antiviral Research

journal homepage: www.elsevier.com/locate/antiviral

Novel screening systems for HIV-1 fusion mediated by two extra-virion heptad repeats of gp41

Hiroki Nishikawa[a], Eiichi Kodama[b,*], Ayako Sakakibara[b], Ayako Fukudome[b], Kazuki Izumi[b], Shinya Oishi[a], Nobutaka Fujii[a], Masao Matsuoka[b]

[a] Graduate School of Pharmaceutical Sciences, Kyoto University, Sakyo-ku, Kyoto 606-8501, Japan
[b] Laboratory of Virus Immunology, Institute for Virus Research, Kyoto University, Sakyo-ku, Kyoto 606-8507, Japan

ARTICLE INFO

Article history:
Received 12 November 2007
Accepted 5 May 2008

Keywords:
HIV-1
Gp41
Fusion
ELISA
Screening
Alkaline phosphatase

ABSTRACT

Entry of human immunodeficiency virus type 1 (HIV-1) into target cells is mediated by its envelope protein gp41 through membrane fusion. Interaction of two extra-virion heptad repeats (HRs) in the gp41 plays a pivotal role in the fusion, and its inhibitor, enfuvirtide (T-20), blocks HIV-1 entry. To identify agents that block HIV-1 fusion, two screening methods based on detection and quantification by the enzyme-linked immunosorbent assay (ELISA) principle have been established. One method uses an alkaline phosphatase (ALP)-conjugated antibody (Ab-ELISA) and the other uses an ALP-fused HR (F-ELISA) to detect and quantify the interaction of the two HRs. The F-ELISA was more simple and rapid, since no ALP-conjugated antibody reaction was required. Both ELISAs detected all the fusion inhibitors tested except for T-20. Interaction of the two HRs was observed in both ELISAs, even in the presence of 10% dimethyl sulfoxide. Ab-ELISA performed best in a pH ranging from 6 to 8, while F-ELISA performed best at a pH ranging from 7 to 8. These results indicate that both established ELISAs are suitable for the identification of HIV-1 fusion inhibitors.

1. Introduction

Combination chemotherapy has been widely used and reduces the mortality caused by HIV-1 infection. During prolonged therapy, however, in some patients, such efficacy is attenuated by the emergence of drug-resistant variants (Calmy et al., 2004). Moreover, combination chemotherapy occasionally induces various adverse effects and may also increase the costs of the therapy. Therefore, development of novel anti-HIV-1 drugs that suppress replication of resistant variants, and are less toxic and less cost is urgently needed.

There are at least two approaches to controlling replication of resistant variants and/or to reducing unfavorable adverse effects induced by the therapy. One approach is the development of anti-HIV-1 drugs which inhibit new targets such as viral integrase (Hazuda et al., 2004) or cellular receptors such as CCR5 (Tagat et al., 2004). Actually, an integrase inhibitor, raltegravir (Grinsztejn et al., 2007), and a CCR5 antagonist, maraviroc (Fätkenheuer et al., 2005) have been approved for clinical application. The other is the development or modification of current drugs that inhibit well-established targets, to make them effective against resistant variants while reducing adverse side-effects. In this study, we focus on the recently established and promising target of virus–cell membrane fusion.

The mechanism of virus–cell membrane fusion has already been disclosed (Eckert and Kim, 2001). Briefly, one of the HIV-1 envelope glycoproteins, gp120, binds to the host cell receptor CD4 and CXCR4 or CCR5, and then, another membrane-spanning protein gp41 in trimer anchors itself to the host cell membrane. After anchoring, heptad repeats 1 and 2 (HR1 and HR2), which are two extra-virion α-helical regions in the gp41, form an anti-parallel 6-helical bundle and lead to fusion of HIV-1 with the host cell membrane. On the basis of this molecular mechanism, compounds which prevent 6-helical bundle formation will be potential HIV-1 fusion inhibitors. Enfuvirtide (T-20) is the first peptide approved and used against HIV-1 variants that are refractory to the effect of reverse transcriptase and protease inhibitors (Lalezari et al., 2003; Lazzarin et al., 2003). Previously, we and others have developed novel potent fusion inhibitors, in the form of gp41 HR2-derived peptides (Bewley et al., 2002; Otaka et al., 2002; Root et al., 2001) (Fig. 1) and small molecules (Cai and Gochin, 2007; Frey et al., 2006). However, no fusion inhibitors, except for T-20, have been approved for clinical use. To screen further potential fusion inhibitors, we have established two simple, rapid and reproducible

* Corresponding author. Tel.: +81 75 751 3986; fax: +81 75 751 3986.
E-mail address: ekodama@virus.kyoto-u.ac.jp (E. Kodama).

0166-3542/$ – see front matter © 2008 Elsevier B.V. All rights reserved.
doi:10.1016/j.antiviral.2008.05.006

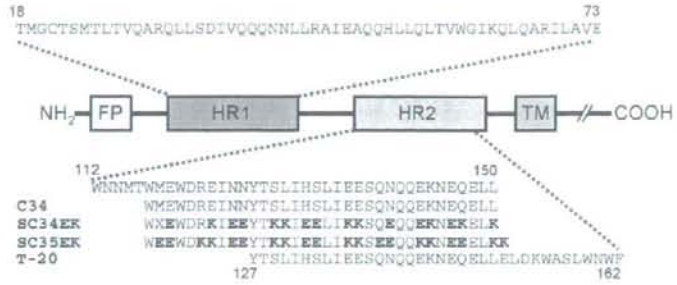

Fig. 1. Schematic view of gp41. The locations of the fusion peptide (FP), N-terminal heptad repeat region (HR1), C-terminal heptad repeat region (HR2), transmembrane domain (TM) and amino acid sequence of HR1, HR2, T-20, C34 and its derivatives (Otaka et al., 2002) are shown. The residue numbers of each peptide correspond to their positions in the envelope protein gp41 of HIV-1 NL4-3 clone. Representative regions of HR1 and HR2 used in this study are defined by the amino acids 18–73 and 112–150, respectively, and designated as MBP-HR1- and GST-HR2- or TRX-ALP-HR2-fused protein as described in Section 2. The X in SC34EK indicates an artificial amino acid norleucine instead of methionine, to avoid oxidation of the methionine residue.

in vitro screening systems using the enzyme-linked immunosorbent assay (ELISA).

2. Materials and methods

2.1. Antiviral agents

The peptide-based fusion inhibitors were synthesized as described previously (Otaka et al., 2002), and their sequences are shown in Fig. 1. CCR5 antagonist TAK-779 (Baba et al., 1999) was provided by Takeda Pharmaceutical Company Ltd. (Osaka, Japan) through an AIDS research and reference reagent program. CXCR4 antagonist AMD-3100 (De Clercq et al., 1994) was provided by S. Shigeta (Fukushima Medical University, Fukushima, Japan). Adsorption inhibitor dextran sulfate MW 5000, DS-5000 (Baba et al., 1988) was purchased from Sigma (St. Louis, MO).

2.2. Protein expression and purification

A DNA fragment of the alkaline phosphatase (ALP) coding region without its secretory signal sequence, corresponding to amino acids 22–471 (Dodt et al., 1986; Kikuchi et al., 1981), was amplified by PCR from the *E. coli* JM109 genome (K12 strain; GenBank accession number: U00096). The amplified ALP region was ligated into the pET32a vector (Novagen, Madison, WI) to create pET32-ALP, a thioredoxin (TRX)-ALP fusion construct. A DNA fragment coding the HR1 region of HIV-1 gp41, amino acid positions 18–73, was amplified by PCR from an HIV-1 molecular clone pNL4-3 (GenBank accession number: AF324493). The amplified HR1 region was ligated into the pMAL-C2 vector (New England Biolabs, Ipswich, MA) to express HR1 with maltose-binding protein (MBP) as a tag, designated pMAL-HR1. The HR2 region, gp41 amino acid positions 112–150, was also amplified and ligated into both the pGEX-5X vector (GE Healthcare, Buckinghamshire, UK) and the pET32-ALP construct to express HR2 fusion protein with glutathione S-transferase (GST) and TRX-ALP, designated pGEX-HR2 and pET32-ALP-HR2, respectively. All vectors were verified by DNA sequencing and transformed into *E. coli* BL21-CodonPlus (DE3)-RIL strain (Stratagene, La Jolla, CA) for bacterial expression. The expressed MBP-HR1, GST-HR2 and TRX-ALP-HR2 proteins were purified by Amylose Resin (New England Biolabs), Glutathione Sepharose 4B (GE Healthcare) and Ni-NTA Agarose (Qiagen, Valencia, CA), respectively, according to the Manufacturers' recommended protocols. Purity was determined by SDS–PAGE and concentration by the Bradford protein assay (Bio-Rad, Hercules, CA).

2.3. Indirect detection of interaction of HR1 and HR2 (Ab-ELISA) (Fig. 2A)

Fifty nanomolar MBP-HR1 dissolved in 50 mM sodium carbonate buffer (pH 9.4) was coated on a 96-well ELISA plate (Costar, Cambridge, MA) by incubation at 4 °C for 8 h. After washing three times with PBS containing 0.025% Tween 20 (T-PBS) (pH 7.4), the plate was blocked using bovine serum albumin (BSA) at a concentration of 1 mg/ml in T-PBS at 4 °C for 2.5 h, and then washed again as described above. The MBP-HR1 on the plate was allowed to bind GST-HR2 (50 nM) by incubation at 37 °C for 1.5 h in the presence or absence of various concentrations of compounds for testing. After washing, binding of GST-HR2 was detected by using alkaline phosphatase (ALP)-conjugated anti-GST antibody (Sigma) in 1:2000 dilution at 4 °C for 1 h, then washed as before, prior to the addition of phosphatase substrate 5-bromo-4-chloro-3-indolyl phosphate (BCIP) (BluePhos Microwell Phosphatase Substrate; KPL, Gaithersburg, MD). After incubating at room temperature for 30 min, absorbance at 595 nm was measured by a plate reader (model 3550, Bio-Rad).

2.4. Direct detection of interaction of HR1 and HR2 (F-ELISA) (Fig. 2D)

All procedures were performed as described above, except that TRX-ALP-HR2 (50 nM) was used in place of GST-HR2, with binding directly detected by BluePhos Microwell Phosphatase Substrate without the interaction of ALP-conjugated anti-GST antibody.

2.5. Anti-HIV activity

Anti-HIV-1 activity was determined by the multinuclear activation of a galactosidase indicator (MAGI) assay as described previously (Kimpton and Emerman, 1992; Kodama et al., 2001). Briefly, the MAGI cells (10^4 cells/well) were seeded in flat bottom 96-well microtitre plates. The following day, the cells were inoculated with HIV-1 and cultured in the presence of various concentrations of inhibitors in fresh medium. After 48 h incubation, all the blue cells stained with 5-bromo-4-chloro-3-indolyl-β-D-galactopyranoside (X-gal) in each well were counted.

3. Results

3.1. Establishment of ELISA

To establish a novel assay system representing the specific interaction of HR1 and HR2 regions of the HIV-1 gp41 protein, a

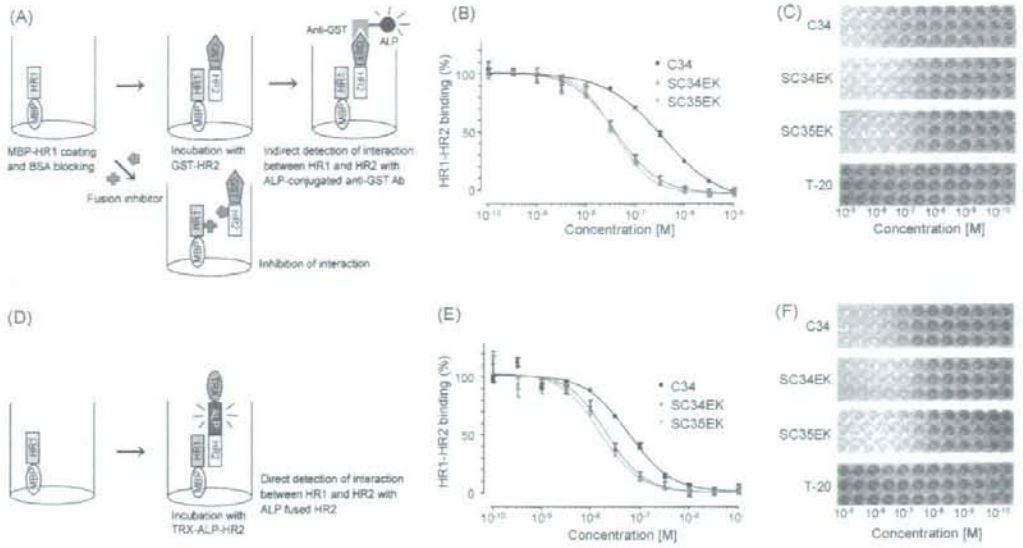

Fig. 2. Flow chart of the established ELISA systems (A and D) and the inhibitory effects of peptide-based fusion inhibitors determined by these systems (B, C, E and F). The schemes of Ab-ELISA and F-ELISA are shown. In Ab-ELISA (A), GST-HR2 interacts with MBP-HR1 on the ELISA plate, and the amounts of GST-HR2 are quantified by using ALP-conjugated anti-GST antibody and ALP substrate. In the presence of fusion inhibitors, GST-HR2 cannot interact with MBP-HR1, resulting in no ALP activity. In F-ELISA (D), ALP-fused HR2 protein enables the detection of the interaction of HR2 directly without ALP-conjugated anti-GST antibody. Inhibition curves of binding by Ab-ELISA (B) and F-ELISA (E) at peptide concentrations 10^{-10} to 10^{-5} M are illustrated. The actual appearance of ELISA plates observed in Ab-ELISA (C) and F-ELISA (F) is shown.

simple ELISA was first established with ALP-conjugated antibody (Ab-ELISA) as shown in Fig. 2A. MBP-HR1 was coated onto a 96-well ELISA plate. After blocking with BSA, GST-HR2 solution was added to the MBP-HR1 coated well. Using ALP-conjugated anti-GST antibody, the interaction of HR1 and HR2 was colorimetrically measured by a plate reader. Agents that block the interaction of HR2 with HR1 can reduce optical density at 595 nm (OD_{595}). The period for efficient coating of MBP-HR1 to the plate was measured by detection of ALP-conjugated anti-MBP antibody. After 8 h and up to 24 h little increase in efficiency of MBP-HR1 coating was observed (data not shown). When coating and blocking were performed prior to the assay, total time of the procedure, excluding washing, was only 3 h.

Prior to evaluation of fusion inhibitors, we examined interaction of GST-HR2 with the MBP-HR1 coating. We first coated MBPs with or without HR1 at a concentration of 50 nM, incubated them with various concentrations of GST-HR2, and then detected bound GST-HR2 with anti-GST antibody. GST-HR2 interacted with MBP-HR1 in a dose-dependent manner, at least up to 100 μM and provided sufficient OD_{595} values, over 1.0 (Fig. 3). Thus, 50 nM of GST-HR2 was used for further experiments.

Next, we modified the Ab-ELISA by using ALP-fused HR2 instead of GST-HR2 in the reaction with coated MBP-HR1, as shown in Fig. 2D (F-ELISA). The ALP-fused HR2 enabled us to directly detect the HR1 and HR2 interaction without the antibody reaction step, thus providing an even more rapid and simple procedure than the Ab-ELISA which uses ALP-conjugated antibody for detection. The total time required for the F-ELISA, excluding coating and blocking, was approximately 2 h. These results demonstrate that the ELISA systems detect the interaction of HR1 and HR2 interaction, enables the screening of potential fusion inhibitors without the need for infectious HIV-1 material, and is both simple and rapid.

3.2. Inhibitory effect of HR2-derived peptides and other entry inhibitors

The efficacy of the fusion inhibitory peptides C34, SC34EK and SC35EK and other compounds was determined by both Ab-ELISA (Fig. 2A) and F-ELISA (Fig. 2D). Both ELISAs only detected the activities of these three fusion inhibitory peptides, but not of other entry inhibitors (Table 1). The inhibitory effects of these peptide fusion inhibitors were reproducible and displayed a sigmoidal dose-dependent curve (Fig. 2B and E). These results suggested that our established ELISAs were specific for the interaction between HR1 and HR2 in the fusion process. Higher sensitivities for peptides tested were obtained by F-ELISA compared with those by Ab-ELISA (Table 1). However, compared with the MAGI assay, sensitivities of both ELISAs were between 14- and 50-fold lower. Neither ELISA technique was able to detect the inhibitory effect of T-20, which

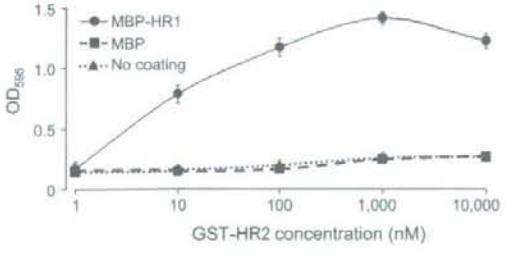

Fig. 3. The binding efficacy of GST-HR2. Fifty nanomolars of MBP-HR1 (circle), MBP (square) and mock (triangle with broken line) were coated on the plate. Various concentrations of GST-HR2 were added and incubated at 37 °C for 1.5 h. Bound GST-HR2 was detected with ALP-conjugated anti-GST antibody by measuring the optical density at 595 nm (OD_{595}).

Table 1
The efficacy of HR2-derived peptides and other entry inhibitors as determined by Ab-ELISA or F-ELISA and the cell-based MAGI assay

Compounds	EC_{50} (nM)[a]			
	Ab-ELISA[b]	F-ELISA[c]	MAGI[d]	
			NL4-3[e]	BaL[f]
C34[g]	365 ± 43	59 ± 7.7	4.0 ± 0.86	N.D.[h]
SC34EK[g]	41 ± 5.0	21 ± 3.2	1.6 ± 0.61	N.D.
SC35EK[g]	38 ± 3.0	16 ± 2.8	0.35 ± 0.030	N.D.
T-20[g]	>10,000	>10,000	35 ± 17	N.D.
TAK-779	>100,000	>100,000	>100,000	1.85 ± 0.19
AMD-3100	>100,000	>100,000	0.39 ± 0.030	>100,000
DS-5000	>100,000	>100,000	19 ± 6.0	348 ± 46

[a] EC_{50} refers to the concentration of peptides which show 50% inhibition relative to the control.
[b] The amount of binding GST-HR2 measured by ALP-conjugated anti-GST antibody.
[c] Direct detection of HR1 and HR2 interaction without antibody reaction by using ALP-fused HR2 protein.
[d] Multinuclear activation of a galactosidase indicator assay using HeLa CD4-LTR/β-galactosidase indicator cells (Kimpton and Emerman, 1992).
[e] CXCR4 (X4) tropic HIV-1 strain.
[f] CCR5 (R5) tropic HIV-1 strain.
[g] Peptide sequences are shown in Fig. 1.
[h] Not determined.

has anti-fusion activity in vitro and in vivo, even though the gp41 amino acid region 23–58, which is a predictive site for T-20 interaction, is included in the MBP-HR1 fusion protein (Figs. 1 and 2C and F; Table 1). We further examined the effect on T-20 susceptibility of changing the coating and interaction. In this experiment, first GST-HR2 was coated, then exposed to MBP-HR1, and finally detected by anti-MBP antibody. Again C34 and its derivatives were effective, but T-20 was not (data not shown).

3.3. Effect of DMSO concentration and pH

For screening, compounds are frequently dissolved in dimethyl sulfoxide (DMSO). However, high concentrations of DMSO (over 1%) reduced cell viability in the cell-based assay, e.g., MAGI assay. The ELISA systems described here do not require cells, thus should be less influenced by DMSO concentration compared to the MAGI assay. To verify this, we determined the concentration of DMSO that affects the interaction of HR1 and HR2 in our ELISAs. In both the Ab-ELISA and F-ELISA, DMSO concentrations up to 10% did not influence the optical densities to any significant extent (Fig. 4A). At these concentrations, optical densities recorded were less than 20% lower compared to those recorded in the absence of DMSO, indicating that the sensitivities of these tests would be sufficient to screen compounds that are dissolved in reagents containing up to 10% DMSO.

Next, we investigated the effect of pH on detection by ELISA. High concentrations of some compounds that are highly acidic or basic may decrease viability of the cells in cell-based assays. The pH of the reaction buffer was modified by addition of HCl and NaOH as control acidic or basic compounds, respectively. In the F-ELISA, binding of HR1 and HR2 was 2–2.5-fold greater at pH less than 7 than at pH 7.4, while in the Ab-ELISA, the binding was relatively stable at pH 6 (Fig. 4B) and reduction of HR1 and HR2 binding was less than 20%. On the other hand, at basic pH, binding of HR1 and HR2 were relatively stable up to pH 9 in both ELISAs. These results indicate that both systems are less influenced by DMSO concentrations up to 10% and in basic reaction conditions compared to cell-based assays. However, in acidic reaction conditions, interaction of HR1 and HR2 is likely to be overestimated in the F-ELISA.

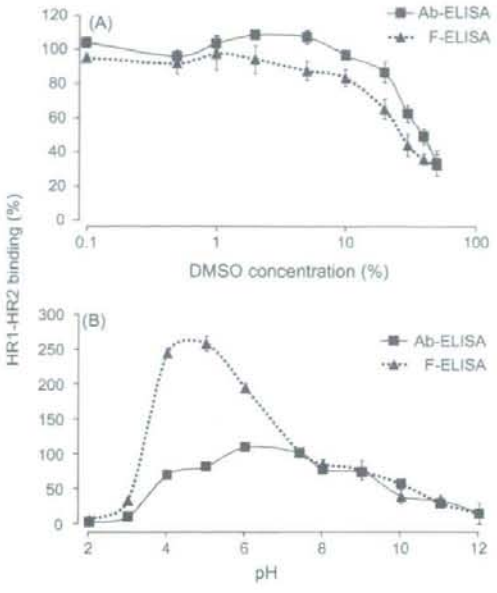

Fig. 4. Effects of DMSO concentration and pH. The effect of DMSO from 0.1 to 50% added to the reaction of HR1 and HR2 is shown (A). Binding is expressed as a percentage of that in the absence of DMSO. Alteration of the pH from 2 to 12 at the HR1 and HR2 reaction was performed by using HCl or NaOH (B). Binding is expressed as a percentage of that at pH 7.4.

4. Discussion

Our newly established ELISA systems successfully detected the HIV-fusion inhibitory activities of C34, a peptide-based fusion inhibitor (Fig. 1), and its derivatives in a dose-dependent manner. However, T-20 lacking the N-terminal 10 amino acids of C34 but containing an additional 12 amino acids in the C-terminal region did not show activity in either of the ELISA systems (Fig. 2; Table 1). T-20 is believed to inhibit 6-helical bundle formation through competition with the physiological HR2 region of gp41. This hypothesis is strongly supported by the introduction of a site of mutations for T-20 resistance in vivo. Variants isolated from T-20 treated patients frequently display mutations in the HR1 region, especially at amino acids 36–45, including D36G/V/S, V38A/E and N43D (Aquaro et al., 2006; Cabrera et al., 2006; Mink et al., 2005; Poveda et al., 2002; Rimsky et al., 1998; Wei et al., 2002) (Fig. 1). Interestingly, amino acid positions 36–45 are also crucial for C34 binding, and some C34 resistant variants also show cross-resistance to T-20 (Nameki et al., 2005). Moreover, our preliminary data in the time course of addition experiments showed that the profile of inhibition is identical between C34 and T-20 (data not shown).

Our designed MBP-HR1 contains the presumed interaction site of T-20 (amino acid positions 23–58), as determined by crystal structure analysis of the N36–C34 complex (Chan et al., 1997) (Fig. 1). However, we failed to detect T-20 inhibitory activity in our ELISA systems (Fig. 2C and F). To the best of our knowledge, there are no reports that describe the potent activity of T-20 in protein- or peptide-based assays (Cai and Gochin, 2007; Huang et al., 2006, 2007; Jiang et al., 1999; Liu et al., 2007; Ryu et al., 1998; Xu et al., 2007).

In this regard, two groups have tried to reveal the mechanism of action of T-20 mainly through physicochemical experiments, with both groups proposing that T-20 may act through the lipid mem-

brane. Jiang et al. has proposed that HR2 peptides have two different functional domains, an HR1-binding domain, and a lipid-binding domain (Liu et al., 2007). C34 contains an HR1-binding sequence but not a lipid-binding domain, while T-20 has only a lipid-binding domain, suggesting that T-20 might be functional only in the presence of lipid membrane. Wexler-Cohen and Shai (2007), also found that the C-terminal region of T-20 which was not included in C34 could be replaced with fatty acid, indicating that T-20 acts through the lipid membrane.

It is possible that MBP hampers the proper conformation of HR1. However, in the 6-helix bundle crystal structure of human T cell leukemia virus type 1 gp21, MBP remained fused to the N-terminal of HR1 (Kobe et al., 1999). Thus, it is unlikely that the inability of HR1 to bind T-20 is due to improper conformation of HR1. Moreover, even synthetic peptides of HR1 and T-20 do not bind each other (Liu et al., 2005).

To date, several peptide-based detection systems have been reported, although they failed to demonstrate T-20 activity. Most of them utilize the NC-1 monoclonal antibody which recognizes discontinuous epitopes presented on the 6-helix complex between N36 and C34 to detect 6-helical conformations (Huang et al., 2006, 2007; Jiang et al., 1999; Liu et al., 2007). It is predicted that this system may not detect the peptide-based fusion inhibitor C34 itself or may not detect C34 derivatives, since the antibody NC-1 was derived from the 6-helix conformation of N36 and C34 peptides. Ryu et al. (1998) also reported similar ELISA systems, but showed an inhibitory effect only for C51 with an EC_{50} value of 1.0 μg/ml (approximately 200 nM). Other groups have reported the development of assay systems using fluorescence resonance energy transfer (FRET) (Cai and Gochin, 2007; Xu et al., 2007). Although FRET requires no coating and washing steps, it seems to be less sensitive compared to our ELISA systems. In fact, EC_{50} values of C34 in the FRET system were described as approximately 5 μM (Xu et al., 2007), while those in our Ab-ELISA and F-ELISA were 365 and 59 nM, respectively (Table 1).

The sensitivities of our ELISA systems were lower than those of the cell-based MAGI assay (Table 1). However, the ELISA systems could detect the interaction between HR1 and HR2 even at a high concentration of DMSO, and in a relatively wide pH range (Fig. 4), indicating their capacity for screening of highly concentrated compounds. Decreased concentrations of MBP-HR1 and GST-HR2 or ALP-HR2 increased the antiviral sensitivity, although this also reduced detection sensitivity of ALP activity. Detection sensitivity could be increased by using a highly sensitive chemiluminescent probe as an alternative to the BCIP substrate we used.

At pH greater than 8, both ELISAs showed decreased optical density, while at pH less than 7, enhanced ALP activity was observed in F-ELISA compared with the neutral pH 7.4 (Fig. 4B). Although we could not elucidate the detailed mechanism at present, even in Ab-ELISA, the optical density was also enhanced by using an acidic buffer in the incubation of GST-HR2 with anti-GST antibody (data not shown). Thus, low pH enhances ALP activity rather than enhancing the interaction of HR1 and HR2. These results indicate that we should take note of this artificial enhancement when acidic compounds are screened by F-ELISA.

Major difference between class I and class II fusion is based upon the structure of the glycoproteins involved in the fusion process. For instance, HIV and FluV utilize alpha-helix structure domains located in gp41 and HA2, respectively. In contrast, Flaviviruses, which fuse through class II, utilize beta-sheet structure domains in E protein. Although both glycoproteins complete fusion with trimer of hairpins (alpha-helix and beta-sheet, respectively), in the pre-fusion state, they form trimers and dimers, for class I and class II, respectively. Moreover, the fusion peptide domain which is directly inserted into target cell membrane, is located at N-terminus and internal loop of the env-protein, for class I and class II, respectively.

At the virus–cell membrane fusion step, the interaction between viral envelope proteins HR1 and HR2 is a common mechanism of class I fusion (Jahn et al., 2003; Schibli and Weissenhorn, 2004). It is expected that establishment of a similar ELISA screening system for other viruses using class I fusion for cell entry, such as influenza virus (Eckert and Kim, 2001), feline immunodeficiency virus (FIV) (Medinas et al., 2002), severe acute respiratory syndrome coronavirus (SARS-CoV) (Bosch et al., 2004) and Ebola virus (Watanabe et al., 2000) is possible. For some highly virulent agents, such as SARS-CoV and Ebola virus, our system will be an extremely useful tool since it does not require infectious material.

In this study, we have developed two novel in vitro assay systems for fusion inhibitors by focusing on the interaction of envelope proteins HR1 and HR2. Hydrophobic pocket in HR1 and tryptophan rich domain in HR2 acting as "pocket" and "knob", respectively, play a key role in the virus–cell membrane fusion process, indicating that these interactions are an attractive target for small molecule fusion inhibitors (Ferrer et al., 1999). C34, GST-HR2 and ALP-TRX-HR2 used in this study contain "knob" region but T-20 does not. The developed systems are also ideal for initial screenings because of low variability and good reproducibility even at high compound concentration, and since they allow for a non-infectious rapid and simple procedure. These assays will be useful for the discovery of novel fusion inhibitors not only of HIV-1, but also of other viruses which utilize the class I fusion mechanism.

Acknowledgements

This work was supported in part by grants for the Promotion of AIDS Research from the Ministry of Health and Welfare and the Ministry of Education, Culture, Sports, Science, and Technology of Japan (E.K. and S.O.); a grant for Research for Health Sciences Focusing on Drug Innovation from The Japan Health Sciences Foundation (E.K., S.O., N.F. and M.M.); and the 21st Century COE program "Knowledge Information Infrastructure for Genome Science" (N.F. and H.N.). H.N. is grateful for the JSPS Research Fellowships for Young Scientists. Appreciation is expressed to Mr. Maxwell Reback (Kyoto University) for reading the manuscript.

References

Aquaro, S., D'Arrigo, R., Svicher, V., Perri, G.D., Caputo, S.L., Visco-Comandini, U., Santoro, M., Bertoli, A., Mazzotta, F., Bonora, S., Tozzi, V., Bellagamba, R., Zaccarelli, M., Narciso, P., Antinori, A., Perno, C.F., 2006. Specific mutations in HIV-1 gp41 are associated with immunological success in HIV-1-infected patients receiving enfuvirtide treatment. J. Antimicrob. Chemother. 58, 714–722.

Baba, M., Nishimura, O., Kanzaki, N., Okamoto, M., Sawada, H., Iizawa, Y., Shiraishi, M., Aramaki, Y., Okonogi, K., Ogawa, Y., Meguro, K., Fujino, M., 1999. A small-molecule, nonpeptide CCR5 antagonist with highly potent and selective anti-HIV-1 activity. Proc. Natl. Acad. Sci. U.S.A. 96, 5698–5703.

Baba, M., Pauwels, R., Balzarini, J., Arnout, J., Desmyter, J., De Clercq, E., 1988. Mechanism of inhibitory effect of dextran sulfate and heparin on replication of human immunodeficiency virus in vitro. Proc. Natl. Acad. Sci. U.S.A. 85, 6132–6136.

Bewley, C.A., Louis, J.M., Ghirlando, R., Clore, G.M., 2002. Design of a novel peptide inhibitor of HIV fusion that disrupts the internal trimeric coiled-coil of gp41. J. Biol. Chem. 277, 14238–14245.

Bosch, B.J., Martina, B.E., Van Der Zee, R., Lepault, J., Haijema, B.J., Versluis, C., Heck, A.J., De Groot, R., Osterhaus, A.D., Rottier, P.J., 2004. Severe acute respiratory syndrome coronavirus (SARS-CoV) infection inhibition using spike protein heptad repeat-derived peptides. Proc. Natl. Acad. Sci. U.S.A. 101, 8455–8460.

Cabrera, C., Marfil, S., García, E., Martínez-Picado, J., Bonjoch, A., Bofill, M., Moreno, S., Ribera, E., Domingo, P., Clotet, B., Ruiz, L., 2006. Genetic evolution of gp41 reveals a highly exclusive relationship between codons 36, 38 and 43 in gp41 under long-term enfuvirtide-containing salvage regimen. AIDS 20, 2075–2080.

Cai, L., Gochin, M., 2007. A novel fluorescence intensity screening assay identifies new low-molecular-weight inhibitors of the gp41 coiled-coil domain of human immunodeficiency virus type 1. Antimicrob. Agents Chemother. 51, 2388–2395.

Calmy, A., Pascual, F., Ford, N., 2004. HIV drug resistance. N. Engl. J. Med. 350, 2720–2721.

Chan, D.C., Fass, D., Berger, J.M., Kim, P.S., 1997. Core structure of gp41 from the HIV envelope glycoprotein. Cell 89, 263–273.

De Clercq, E., Yamamoto, N., Pauwels, R., Balzarini, J., Witvrouw, M., De Vreese, K., Debyser, Z., Rosenwirth, B., Peichl, P., Datema, R., et al., 1994. Highly potent and selective inhibition of human immunodeficiency virus by the bicyclam derivative JM3100. Antimicrob. Agents Chemother. 38, 668–674.

Dodt, J., Schmitz, T., Schäfer, T., Bergmann, C., 1986. Expression, secretion and processing of hirudin in *E. coli* using the alkaline phosphatase signal sequence. FEBS Lett. 202, 373–377.

Eckert, D.M., Kim, P.S., 2001. Mechanisms of viral membrane fusion and its inhibition. Annu. Rev. Biochem. 70, 777–810.

Fätkenheuer, G., Pozniak, A.L., Johnson, M.A., Plettenberg, A., Staszewski, S., Hoepelman, A.I., Saag, M.S., Goebel, F.D., Rockstroh, J.K., Dezube, B.J., Jenkins, T.M., Medhurst, C., Sullivan, J.F., Ridgway, C., Abel, S., James, I.T., Youle, M., van der Ryst, E., 2005. Efficacy of short-term monotherapy with maraviroc, a new CCR5 antagonist, in patients infected with HIV-1. Nat. Med. 11, 1170–1172.

Ferrer, M., Kapoor, T.M., Strassmaier, T., Weissenhorn, W., Skehel, J.J., Oprian, D., Schreiber, S.L., Wiley, D.C., Harrison, S.C., 1999. Selection of gp41-mediated HIV-1 cell entry inhibitors from biased combinatorial libraries of non-natural binding elements. Nat. Struct. Biol. 6, 953–960.

Frey, G., Rits-Volloch, S., Zhang, X.Q., Schooley, R.T., Chen, B., Harrison, S.C., 2006. Small molecules that bind the inner core of gp41 and inhibit HIV envelope-mediated fusion. Proc. Natl. Acad. Sci. U.S.A. 103, 13938–13943.

Grinsztejn, B., Nguyen, B.Y., Katlama, C., Gatell, J.M., Lazzarin, A., Vittecoq, D., Gonzalez, C.J., Chen, J., Harvey, C.M., Isaacs, R.D., 2007. Safety and efficacy of the HIV-1 integrase inhibitor raltegravir (MK-0518) in treatment-experienced patients with multidrug-resistant virus: a phase II randomised controlled trial. Lancet 369, 1261–1269.

Hazuda, D.J., Young, S.D., Guare, J.P., Anthony, N.J., Gomez, R.P., Wai, J.S., Vacca, J.P., Handt, L., Motzel, S.L., Klein, H.J., Dornadula, G., Danovich, R.M., Witmer, M.V., Wilson, K.A., Tussey, L., Schleif, W.A., Gabryelski, L.S., Jin, L., Miller, M.D., Casimiro, D.R., Emini, E.A., Shiver, J.W., 2004. Integrase inhibitors and cellular immunity suppress retroviral replication in rhesus macaques. Science 305, 528–532.

Huang, J.H., Liu, Z.Q., Liu, S., Jiang, S., Chen, Y.H., 2006. Identification of the HIV-1 gp41 core-binding motif—HXXNPF. FEBS Lett. 580, 4807–4814.

Huang, J.H., Yang, H.W., Liu, S., Li, J., Jiang, S., Chen, Y.H., 2007. The mechanism by which molecules containing the HIV gp41 core-binding motif HXXNPF inhibit HIV-1 envelope glycoprotein-mediated syncytium formation. Biochem. J. 403, 565–571.

Jahn, R., Lang, T., Südhof, T.C., 2003. Membrane fusion. Cell 112, 519–533.

Jiang, S., Lin, K., Zhang, L., Debnath, A.K., 1999. A screening assay for antiviral compounds targeted to the HIV-1 gp41 core structure using a conformation-specific monoclonal antibody. J. Virol. Methods 80, 85–96.

Kikuchi, Y., Yoda, K., Yamasaki, M., Tamura, G., 1981. The nucleotide sequence of the promoter and the amino-terminal region of alkaline phosphatase structural gene (phoA) of *Escherichia coli*. Nucl. Acids Res. 9, 5671–5678.

Kimpton, J., Emerman, M., 1992. Detection of replication-competent and pseudotyped human immunodeficiency virus with a sensitive cell line on the basis of activation of an integrated beta-galactosidase gene. J. Virol. 66, 2232–2239.

Kobe, B., Center, R.J., Kemp, B.E., Poumbourios, P., 1999. Crystal structure of human T cell leukemia virus type 1 gp21 ectodomain crystallized as a maltose-binding protein chimera reveals structural evolution of retroviral transmembrane proteins. Proc. Natl. Acad. Sci. U.S.A. 96, 4319–4324.

Kodama, E.I., Kohgo, S., Kitano, K., Machida, H., Gatanaga, H., Shigeta, S., Matsuoka, M., Ohrui, H., Mitsuya, H., 2001. 4′-Ethynyl nucleoside analogs: potent inhibitors of multidrug-resistant human immunodeficiency virus variants in vitro. Antimicrob. Agents Chemother. 45, 1539–1546.

Lalezari, J.P., Henry, K., O'Hearn, M., Montaner, J.S., Piliero, P.J., Trottier, B., Walmsley, S., Cohen, C., Kuritzkes, D.R., Eron Jr., J.J., Chung, J., DeMasi, R., Donatacci, L., Drobnes, C., Delehanty, J., Salgo, M., 2003. Enfuvirtide, an HIV-1 fusion inhibitor, for drug-resistant HIV infection in North and South America. N. Engl. J. Med. 348, 2175–2185.

Lazzarin, A., Clotet, B., Cooper, D., Reynes, J., Arasteh, K., Nelson, M., Katlama, C., Stellbrink, H.J., Delfraissy, J.F., Lange, J., Huson, L., DeMasi, R., Wat, C., Delehanty, J., Drobnes, C., Salgo, M., 2003. Efficacy of enfuvirtide in patients infected with drug-resistant HIV-1 in Europe and Australia. N. Engl. J. Med. 348, 2186–2195.

Liu, S., Jing, W., Cheung, B., Lu, H., Sun, J., Yan, X., Niu, J., Farmar, J., Wu, S., Jiang, S., 2007. HIV gp41 C-terminal heptad repeat contains multifunctional domains. Relation to mechanisms of action of anti-HIV peptides. J. Biol. Chem. 282, 9612–9620.

Liu, S., Lu, H., Niu, J., Xu, Y., Wu, S., Jiang, S., 2005. Different from the HIV fusion inhibitor C34, the anti-HIV drug Fuzeon (T-20) inhibits HIV-1 entry by targeting multiple sites in gp41 and gp120. J. Biol. Chem. 280, 11259–11273.

Medinas, R.J., Lambert, D.M., Tompkins, W.A., 2002. C-terminal gp40 peptide analogs inhibit feline immunodeficiency virus: cell fusion and virus spread. J. Virol. 76, 9079–9086.

Mink, M., Mosier, S.M., Janumpalli, S., Davison, D., Jin, L., Melby, T., Sista, P., Erickson, J., Lambert, D., Stanfield-Oakley, S.A., Salgo, M., Cammack, N., Matthews, T., Greenberg, M.L., 2005. Impact of human immunodeficiency virus type 1 gp41 amino acid substitutions selected during enfuvirtide treatment on gp41 binding and antiviral potency of enfuvirtide in vitro. J. Virol. 79, 12447–12454.

Nameki, D., Kodama, E., Ikeuchi, M., Mabuchi, N., Otaka, A., Tamamura, H., Ohno, M., Fujii, N., Matsuoka, M., 2005. Mutations conferring resistance to human immunodeficiency virus type 1 fusion inhibitors are restricted by gp41 and Rev-responsive element functions. J. Virol. 79, 764–770.

Otaka, A., Nakamura, M., Nameki, D., Kodama, E., Uchiyama, S., Nakamura, S., Nakano, H., Tamamura, H., Kobayashi, Y., Matsuoka, M., Fujii, N., 2002. Remodeling of gp41-C34 peptide leads to highly effective inhibitors of the fusion of HIV-1 with target cells. Angew. Chem. Int. Ed. Engl. 41, 2937–2940.

Poveda, E., Rodés, B., Toro, C., Martin-Carbonero, I., Gonzalez-Lahoz, J., Soriano, V., 2002. Evolution of the gp41 env region in HIV-infected patients receiving T-20, a fusion inhibitor. AIDS 16, 1959–1961.

Rimsky, L.T., Shugars, D.C., Matthews, T.J., 1998. Determinants of human immunodeficiency virus type 1 resistance to gp41-derived inhibitory peptides. J. Virol. 72, 986–993.

Root, M.J., Kay, M.S., Kim, P.S., 2001. Protein design of an HIV-1 entry inhibitor. Science 291, 884–888.

Ryu, J.R., Lee, J., Choo, S., Yoon, S.H., Woo, E.R., Yu, Y.G., 1998. Development of an in vitro assay system for screening of gp41 inhibitory compounds. Mol. Cells 8, 717–723.

Schibli, D.J., Weissenhorn, W., 2004. Class I and class II viral fusion protein structures reveal similar principles in membrane fusion. Mol. Membr. Biol. 21, 361–371.

Tagat, J.R., McCombie, S.W., Nazareno, D., Labroli, M.A., Xiao, Y., Steensma, R.W., Strizki, J.M., Baroudy, B.M., Cox, K., Lachowicz, J., Varty, G., Watkins, R., 2004. Piperazine-based CCR5 antagonists as HIV-1 inhibitors. IV. Discovery of 1-[(4,6-dimethyl-5-pyrimidinyl)carbonyl]-4-[4-[2-methoxy-1(*R*)-4-(trifluoromethyl)phenyl]ethyl-3(*S*)-methyl-1-piperazinyl]-4-methylpiperidine (Sch-417690/Sch-D), a potent, highly selective, and orally bioavailable CCR5 antagonist. J. Med. Chem. 47, 2405–2408.

Watanabe, S., Takada, A., Watanabe, T., Ito, H., Kida, H., Kawaoka, Y., 2000. Functional importance of the coiled-coil of the Ebola virus glycoprotein. J. Virol. 74, 10194–10201.

Wei, X., Decker, J.M., Liu, H., Zhang, Z., Arani, R.B., Kilby, J.M., Saag, M.S., Wu, X., Shaw, G.M., Kappes, J.C., 2002. Emergence of resistant human immunodeficiency virus type 1 in patients receiving fusion inhibitor (T-20) monotherapy. Antimicrob. Agents Chemother. 46, 1896–1905.

Wexler-Cohen, Y., Shai, Y., 2007. Demonstrating the C-terminal boundary of the HIV 1 fusion conformation in a dynamic ongoing fusion process and implication for fusion inhibition. FASEB J. 21, 3677–3684.

Xu, Y., Hixon, M.S., Dawson, P.E., Janda, K.D., 2007. Development of a FRET assay for monitoring of HIV gp41 core disruption. J. Org. Chem. 72, 6700–6707.

Bioorganic & Medicinal Chemistry Letters 18 (2008) 4124–4129

Contents lists available at ScienceDirect

Bioorganic & Medicinal Chemistry Letters

journal homepage: www.elsevier.com/locate/bmcl

Identification of novel non-peptide CXCR4 antagonists by ligand-based design approach

Satoshi Ueda [a], Manabu Kato [a], Shinsuke Inuki [a], Hiroaki Ohno [a], Barry Evans [b], Zi-xuan Wang [b], Stephen C. Peiper [b], Kazuki Izumi [c], Eiichi Kodama [c], Masao Matsuoka [c], Hideko Nagasawa [d], Shinya Oishi [a,*], Nobutaka Fujii [a,*]

[a] Graduate School of Pharmaceutical Sciences, Kyoto University, Sakyo-ku, Kyoto 606-8501, Japan
[b] Department of Pathology, Medical College of Georgia, GA 30912, USA
[c] Institute for Virus Research, Kyoto University, Sakyo-ku, Kyoto 606-8507, Japan
[d] Gifu Pharmaceutical University, Mitahora-higashi, Gifu 502-8585, Japan

ARTICLE INFO

Article history:
Received 6 April 2008
Revised 21 May 2008
Accepted 22 May 2008
Available online 29 May 2008

Keywords:
Chemokine
CXCR4
SDF-1
Anti-HIV
Indole

ABSTRACT

The design and synthesis of novel non-peptide CXCR4 antagonists is described. The peptide backbone of highly potent cyclic peptide-based CXCR4 antagonists was entirely replaced by an indole framework, which was expected to reproduce the disposition of the key pharmacophores consistent with those of potential bioactive conformations of the original peptides. A structure–activity relationship study on a series of modified indoles identified novel small-molecule antagonists having three pharmacophore functional groups through the appropriate linkers.

Chemokines are a family of small proteins with chemotactic and proactivatory effects on leukocytes. Chemokines mediate their biological effects by binding to the specific G-protein coupled receptor subtypes that are differentially and widely expressed in blood cells. Among these chemokine receptors, CXCR4 has a broad tissue distribution and the activation by its endogenous ligand CXCL12 (SDF-1, stromal cell-derived factor 1) leads to chemotaxis, immunomodulation, and other regulatory functions including progenitor cell migration during embryologic development of the cardiovascular, hematopoietic, and central nervous systems. In addition to its physiological roles, CXCR4 also plays important roles in pathological conditions. These include tumor growth and metastasis[1] and rheumatoid arthritis (RA).[2] CXCR4 has also been reported to act as a major co-receptor involved in the entry of T-cell-line-tropic human immunodeficiency virus type 1 (HIV-1) strains into target cells.[3] Thus, CXCR4 is considered as an important therapeutic target for multiple diseases. Inhibitory compounds of CXCL12 or HIV-1 binding to CXCR4 could be novel classes of anti-cancer, anti-RA, and anti-HIV-1 drugs. Previously, we found highly potent peptide-based CXCR4 antagonists such as **1**, **2**, and **3** (Fig. 1).[4,5]

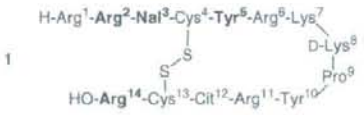

Figure 1. Structures of **1** and its downsized peptides **2** and **3**. Bold residues are the indispensable residues for the potent CXCR4-antagonistic activity. Nal, L-3-(2-naphthyl)alanine; Cit, L-citrulline.

Peptide **1** and its derivatives effectively blocked X4-HIV-1 entry to the cell by specifically binding to CXCR4,[6] and also showed an anti-metastatic effect against breast cancer[7] and anti-RA activity[8] in mouse models.

Although peptides are excellent lead molecules for development of pharmaceutical agents, special drug delivery systems are usually required for their clinical use because of the poor bioavailability and instability against enzymes. Whereas several peptide-based CXCR4 antagonists have been reported, only small numbers of small-molecule CXCR4 antagonists have been

* Corresponding authors. Tel: +81 75 753 4551; fax: +81 75 753 4570 (N. Fujii).
E-mail addresses: soishi@pharm.kyoto-u.ac.jp (S. Oishi), nfujii@pharm.kyoto-u.ac.jp (N. Fujii).

0960-894X/$ - see front matter © 2008 Elsevier Ltd. All rights reserved.
doi:10.1016/j.bmcl.2008.05.092

reported.[9] These prompted us to design novel non-peptide CXCR4 antagonists based on the SAR and conformational studies on peptide ligands **1–3**.

Cyclic pentapeptide-based CXCR4 antagonists **2** and **3** were identified by screening of cyclic pentapeptide libraries, which were designed based on SAR studies of peptide **1**. The constrained backbone of the cyclic peptide was utilized as a template for positioning the key functional groups in space as is found in parent peptide **1**. Subsequent conformational analysis of **2** permitted us to determine the topology of the four indispensable residues, then, rational approach toward the de novo design of non-peptide antagonists may be envisaged.[10]

Our previous SAR studies on **2** and its derivatives have shown that at least three functional groups on the peptide side-chains are required: (1) an aromatic ring such as 2-naphthyl- or 3-indolyl group at position 4; (2) a guanidino group at position 3; (3) a guanidino group at position 2 or a phenol group at position 1.[11] However, it was difficult to determine the spatial relationships between these functional groups due to the free rotation of the side-chain torsion (χ) angles. In our structural analyses, peptide **2** adopted a

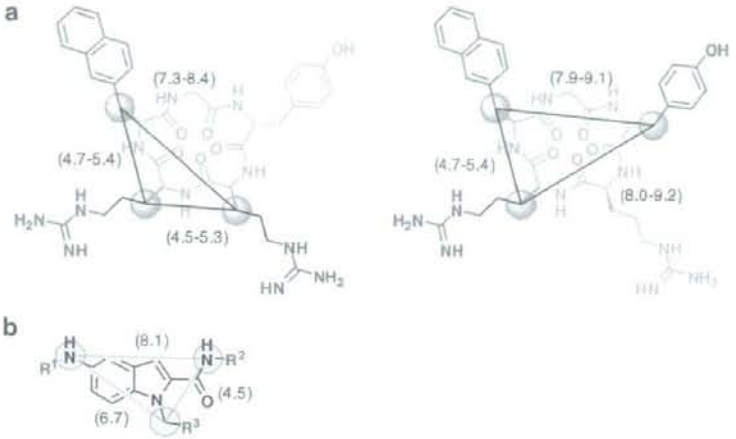

Figure 2. Design of indole-based CXCR4 antagonists based on molecular dynamics calculation of **2**. Distances (Å) between Cβ atoms bearing three essential functional groups during 1000 ps MD calculation of **2** (a) and between two key atoms of energy-minimized 5-acetamido-1-methylindole-2-carboxamide (b) are shown in parentheses. R^1–R^3 include naphthyl, indolyl, guanidino, and phenol groups.

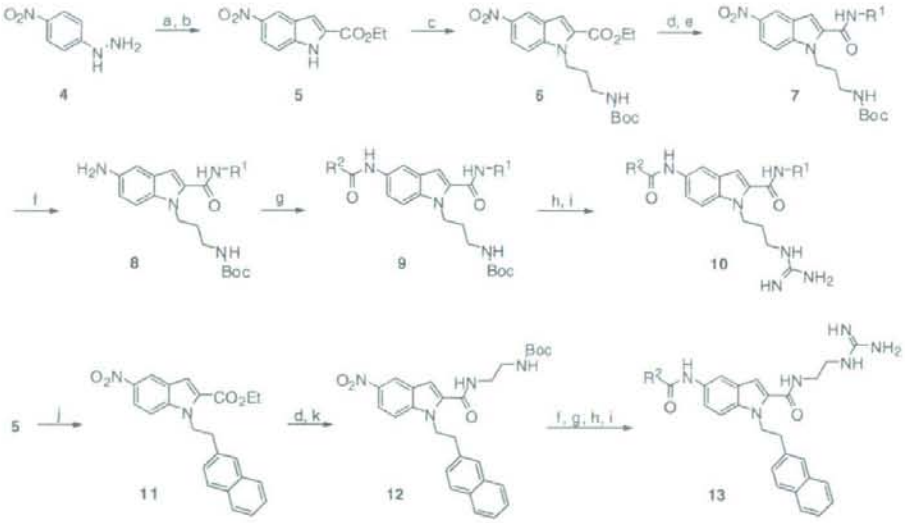

Scheme 1. Reagents and conditions; (a) ethyl pyruvate, EtOH, reflux; (b) polyphosphoric acid, xylene, 130 °C; (c) NaH, *N*-Boc-3-bromopropylamine, DMF, 70 °C; (d) 1 N NaOH aq., EtOH-THF; (e) R^1-NH_2, HATU, Et_3N, DMF; (f) NH_4CO_2H, Pd/C, EtOH-THF, reflux; (g) R^2-CO_2H, HATU, Et_3N, DMF; (h) 95% TFA-H_2O; (i) 1-*H*-pyrazolecarboxamidine hydrochloride, Et_3N, DMF; (j) 2-(2-naphthyl)ethyl bromide, NaH, DMF, 70 °C; (k) *N*-Boc-ethylenediamine, HATU, Et_3N, DMF.

variety of global conformations, in which the distances between indispensable functional groups were variable. On the other hand, relatively rigid cyclic peptide backbone and fixed distances between Cβ atoms, which append key functional groups, were observed.[5] Hence, we envisioned that introduction of crucial functional moieties for receptor binding onto a bicyclic heterocycle scaffold, which mimics the relatively fixed cyclic pentapeptide backbone of **2**, would provide non-peptide CXCR4 ligands. In this letter, we report a part of our ongoing research to develop novel non-peptide small molecule CXCR4 antagonists.

Among several molecular scaffold candidates, we first selected 5-aminoindole-2-carboxylic acid for the following reasons: (1) molecular modeling suggested that it met the spatial requirements for displaying the three key substituents (Fig. 2);[12] (2) accessible synthetic approaches were available for attachment of the three substituents; (3) indoles represent an important class of bioactive compounds and the physicochemical properties in terms of medicinal chemistry are well-documented.

Syntheses of indole-based compounds were achieved as shown in Scheme 1. (4-Nitrophenyl)hydrazine **4** was converted to the corresponding hydrazone, which was subjected to Fischer ring closure reaction to produce an indole **5**. Alkylation of N^1 position of the indole **5** with *N*-Boc-3-bromopropylamine gave **6**. This was hydrolyzed using 1 N aqueous sodium

Table 1
Inhibitory activities of indole derivatives **10a–j** and **13a–b** against binding of ^{125}I-SDF-1α to CXCR4

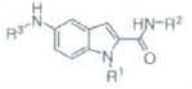

Compound	R^1	R^2	R^3	% inhibition at 10 μM
10a	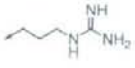	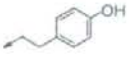	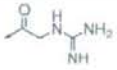	23
10b	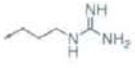	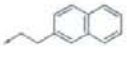	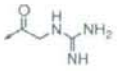	63
10c	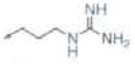	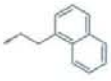	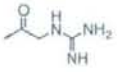	61
10d	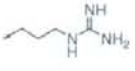	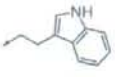	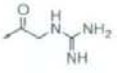	88
10e	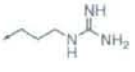	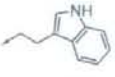	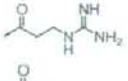	70
10f	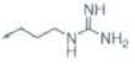	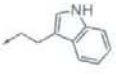	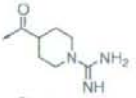	86
10g[a]	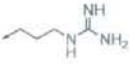	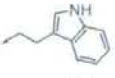	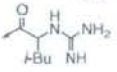	77
10h[a]	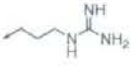	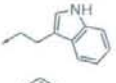	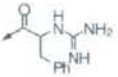	72
10i	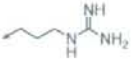		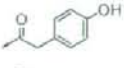	62
10j	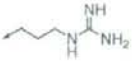		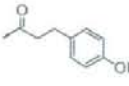	55
13a	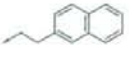	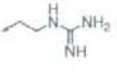	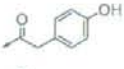	51
13b	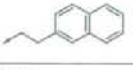	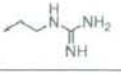	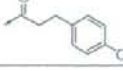	53

[a] Evaluated as a racemic mixture.

hydroxide in EtOH-THF and the resulting free carboxylic acid was coupled with amines using *O*-(7-azabenzotriazol-1-yl)-1,1,3,3-tetramethyluronium hexafluorophosphate (HATU) as coupling reagent to give **7**. The nitro group of **7** was reduced to amine **8** upon treatment with Pd-C and ammonium formate in EtOH. The aminoindole **8** was then coupled with carboxylic acids to give **9**. Deprotection of Boc group(s) by 95% TFA and guanylation of the free amino group(s) produced the target compounds **10**. Another series of compounds **13** were synthesized from **5** using similar reaction sequences described for **10**.

All indole-based compounds listed in Tables 1 and 2 were purified by preparative reverse-phase HPLC (purity >95%) and characterized by MALDI-TOF-MS. These compounds were tested for competitive binding inhibition in human CXCR4 transfected Chinese hamster ovary (CHO) cells using [^{125}I]SDF-1 as a radioligand, with the results given as percentage inhibition at 10 μM. IC_{50} values of selected compounds are shown in Table 2.

Compound **10d** with 2-(3-indolyl)ethyl group at the R^2 position showed 88% inhibition at 10 μM (IC_{50} = 3.0 μM) and was more potent than compounds having (4-hydroxyphenyl)-, (1-naphthyl)- or (2-naphthyl)-alkyl group at the R^2 position (compounds **10a–c**, 23–63% inhibition at 10 μM). Further SAR studies based on **10d** were undertaken. Chain elongation of the guanidinoacetyl group (R^3) of **10d** caused slight decrease in the affinity (**10e**). The use of *N*-amidinopiperidine-4-carbonyl was also acceptable for high potency [IC_{50} (**10f**) = 3.0 μM]. Introduction of an isobutyl or benzyl group into the α-carbon of guanidinomethyl carbonyl group of **10d** did not cause significant drop in binding affinity (compounds **10g** and **10h**). Compounds with *S*-configuration at the chiral center showed more potent CXCR4 antagonistic activity as compared with the corresponding *R*-isomers. (***S***)-**10g** was identified as the most potent compound [IC_{50} ((***S***)-**10g**) = 1.2 μM].[13] Compound (***S***)-**10g** also showed potent anti-HIV-1 activity (IIIB strain, inhibition of HIV-1 induced cytopathogenicity; EC_{50} = 5.4 μM). The IC_{50} value of (***S***)-**10g** is 34-fold lower as compared with parent peptide **2**. This is probably due to the absence of phenol functionality in (***S***)-**10g** which corresponds to D-Tyr side-chain of peptide **2**. Decreased number of amide bond in (***S***)-**10g** might also lead to the lower affinity. We have previously showed the importance of backbone amide functionalities of **2** for CXCR4 antagonistic activity by using reduced-amide isosteres or (*E*)-alkene dipeptide isosteres.[14]

Indole-based compounds having a phenol group at R^3 position showed moderate CXCR4-binding affinity (**10i**, **10j**, **13a**, and **13b**). Interestingly, these compounds did not show complete inhibition even at higher concentrations in the binding inhibition experiments, while compounds having a guanidino group at R^3 position (**10c**, **10d**, and (***S***)-**10g**) achieved complete inhibition (Fig. 3). These results suggest that **10c**, **10d** and (***S***)-**10g** are inhibitors that competitively bind to the SDF-1 binding site of CXCR4, while **10i**, **10j**, **13a**, and **13b** may bind to an allosteric site of CXCR4 and partially antagonize the SDF-1 binding.

Comparison of energy-minimized structures of (***S***)-**10g** and previously reported solution conformation of **2** revealed that three functional groups on the indole template well overlapped the three pharmacophore residues of **2** as expected. In this model, indole scaffold favorably mimicked the backbone of Arg–Arg–Nal sequence of **2** (see Fig. 4).

In summary, a series of indole-based compounds were designed, synthesized, and characterized as a novel class of CXCR4 antagonists. Although their IC_{50} values are in the μM range, these indole derivatives could serve as a useful lead for further medicinal chemistry programs.

Table 2
IC_{50} values of selected indole derivatives

Compound	Structure	IC_{50} (μM)
10d	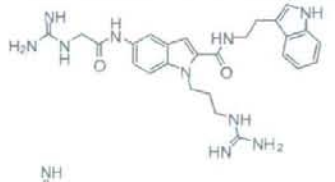	3.0
10f	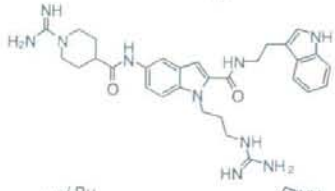	3.0
(*S*)-**10g**	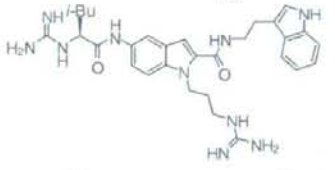	1.2
(*R*)-**10g**	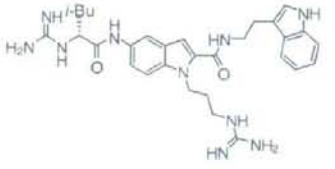	2.2
(*S*)-**10h**	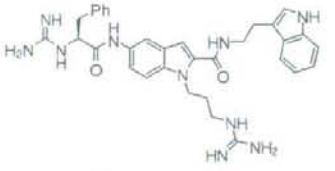	1.7
(*R*)-**10h**	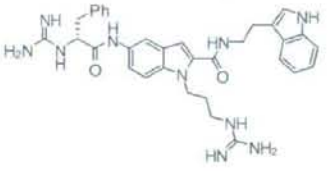	3.7
10i	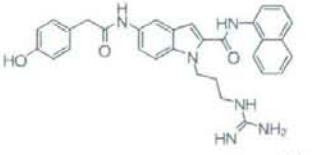	4.8
13b	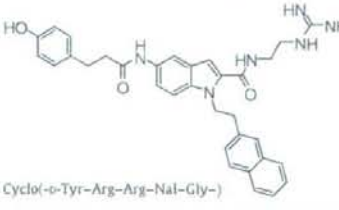	2.7
2	Cyclo(-D-Tyr–Arg–Arg–Nal–Gly–)	0.035

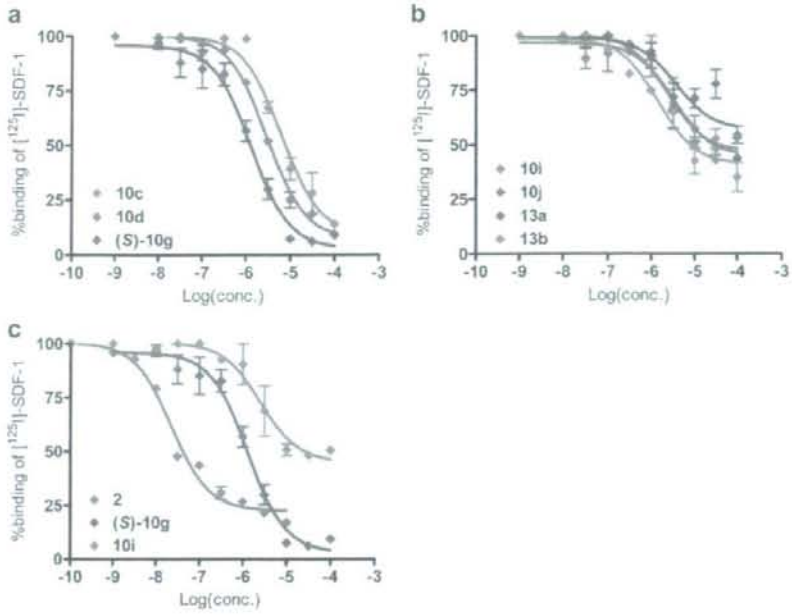

Figure 3. Ligand binding dose response of the compounds (a) having two guanidino pharmacophores and (b) having a phenol pharmacophore, and (c) the comparison of the two subsets with the parent peptide **2**.

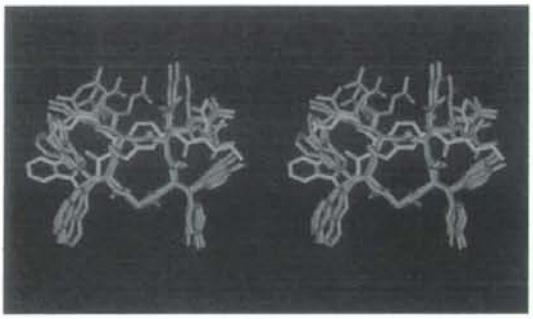

Figure 4. Overlay of a low-energy structure of (*S*)-**10g** (green) and **2** (gray). The molecular modeling of (*S*)-**10g** was performed using MacroModel-Program (Ver. 8.1) with 'MMFF' force field.

Acknowledgments

This work was supported by Grant-in-Aid for Scientific Research and Targeted Proteins Research Program from the Ministry of Education, Culture, Sports, Science, and Technology of Japan, and Health and Labour Sciences Research Grants (Research on HIV/AIDS). Computation time was provided by the Supercomputer Laboratory, Institute for Chemical Research, Kyoto University. S.U. and S.I. are grateful to the JSPS Research Fellowships for Young Scientists.

References and notes

1. Müller, A.; Homey, B.; Soto, H.; Ge, N.; Catron, D.; Buchanan, M. E.; Mcclanahan, T.; Murphy, E.; Yuan, W.; Wagner, S. M.; Barrera, J. L.; Mohar, A.; Verástegui, E.; Zlotnik, A. *Nature* **2001**, *410*, 50.
2. Nanki, T.; Hayashida, K.; El-Gabalawy, H. S.; Suson, S.; Shi, K.; Girschick, H. J.; Yavuz, S.; Lipsky, P. E. *J. Immunol.* **2000**, *165*, 6590.
3. Oberlin, E.; Amara, A.; Bachelerie, F.; Bessia, C.; Virelizier, J. L.; Arenzana-Seisdedos, F.; Schwartz, O.; Heard, J. M.; Clark-Lewis, I.; Legler, D. L.; Loetscher, M.; Baggiolini, M.; Moser, B. *Nature* **1996**, *382*, 833.
4. Masuda, M.; Nakashima, H.; Ueda, T.; Naba, H.; Ikoma, R.; Otaka, A.; Terakawa, Y.; Tamamura, H.; Ibuka, T.; Murakami, T.; Koyanagi, Y.; Waki, M.; Matsumoto, A.; Yamamoto, N.; Funakoshi, S.; Fujii, N. *Biochem. Biophys. Res. Commun.* **1992**, *189*, 845.
5. Fujii, N.; Oishi, S.; Hiramatsu, K.; Araki, T.; Ueda, S.; Tamamura, H.; Otaka, A.; Kusano, S.; Terakubo, S.; Nakashima, H.; Broach, J. A.; Trent, J. O.; Wang, Z.; Peiper, S. C. *Angew. Chem. Int. Ed.* **2003**, *42*, 3251.
6. Tamamura, H.; Xu, Y.; Hattori, T.; Zhang, X.; Arakaki, R.; Kanbara, K.; Omagari, A.; Otaka, A.; Ibuka, T.; Yamamoto, N.; Nakashima, H.; Fujii, N. *Biochem. Biophys. Res. Commun.* **1998**, *253*, 877.
7. (a) Tamamura, H.; Hori, A.; Kanzaki, N.; Hiramatsu, K.; Mizumoto, M.; Nakashima, H.; Yamamoto, N.; Otaka, A.; Fujii, N. *FEBS Lett.* **2003**, *550*, 79; (b) Takenaga, M.; Tamamura, H.; Hiramatsu, K.; Nakamura, N.; Yamaguchi, Y.; Kitagawa, A.; Kawai, S.; Nakashima, H.; Fujii, N.; Igarashi, R. *Biochem. Biophys. Res. Commun.* **2004**, *320*, 226.
8. Tamamura, H.; Fujisawa, M.; Hiramatsu, K.; Mizumoto, M.; Nakashima, H.; Yamamoto, N.; Otaka, A.; Fujii, N. *FEBS Lett.* **2004**, *569*, 99.
9. (a) Donzella, G. A.; Schols, D.; Lin, S. W.; Este, J. A.; Nagashima, K. A.; Maddon, P. J. *Nat. Med.* **1998**, *4*, 72; (b) Ichiya, K.; Yokoyama-Kumakura, S.; Tanaka, Y.; Tanaka, R.; Hirose, K.; Bannai, K.; Edamatsu, T.; Yanaka, M.; Niitani, Y.; Miyano-Kurosaki, N.; Takaku, H.; Koyanagi, Y.; Yamamoto, N. *Proc. Natl. Acad. Sci. U.S.A.* **2003**, *100*, 4185; (c) Tamamura, H.; Ojida, A.; Ogawa, T.; Tsutsumi, H.; Masuno, H.; Nakashima, H.; Yamamoto, N.; Hamachi, I.; Fujii, N. *J. Med. Chem.* **2006**, *49*, 3412; (d) Zhan, W.; Liang, Z.; Zhu, A.; Kurtkaya, S.; Shim, H.; Snyder, J. P.; Liotta, D. C. *J. Med. Chem.* **2007**, *50*, 5655.
10. Conversion of peptide to nonpeptide by scaffolding strategy, see: (a) Hirschmann, R.; Nicolaou, K. C.; Pietranico, S.; Salvino, J.; Leahy, E. M.; Sprengeler, P. A.; Furst, G.; Strader, C. D.; Cascieri, M. A.; Candelore, M. R.; Donaldson; Cindy; Vale, W.; Maechler, L. *J. Am. Chem. Soc.* **1992**, *114*, 9217; (b) Kawato, H. C.; Nakayama, K.; Inagaki, H.; Ohta, T. *Org. Lett.* **2001**, *3*, 3451; (c) Nakayama, K.; Kawato, H. C.; Inagaki, H.; Ohta, T. *Org. Lett.* **2001**, *3*, 3447.
11. (a) Ueda, S.; Oishi, S.; Wang, Z.-x.; Araki, T.; Tamamura, H.; Cluzeau, J.; Ohno, H.; Kusano, S.; Nakashima, H.; Trent, J. O.; Peiper, S. C.; Fujii, N. *J. Med. Chem.* **2007**, *50*, 192; (b) Tamamura, H.; Araki, T.; Ueda, S.; Wang, Z.; Oishi, S.; Esaka, A.; Trent, J. O.; Nakashima, H.; Yamamoto, N.; Peiper, S. C.; Otaka, A.; Fujii, N. *J. Med. Chem.* **2005**, *48*, 3280.
12. Distances (Å) between β-carbons of **2** during 1000 ps MD calculation; D-Tyr^1–Arg^2: 8.0–9.2, D-Tyr^1–Nal^4: 7.9–9.1, Arg^2–Nal^4: 4.7–5.4, Arg^2–Arg^2: 4.5–5.3, Arg^2–Nal^4: 7.3–8.4, Arg^2–Nal^4: 4.7–5.4. Distances (Å) between two key atoms of energy-minimized 5-acetamido-1-methylindole-2-carboxamide:

(acetamide N)-(*N*-methyl C), 6.7; (acetamide N)-(carboxamide N), 8.1; (methyl C)-(carboxamide N), 4.5.

13. Compound (*S*)-**10g**: $[\alpha]_D^{23}$ −6.4(c0.35, CH_3OH); ^1H NMR (500 MHz, DMSO-d_6): δ = 0.93 (d, *J* = 6.0 Hz, 3H), 0.95 (d, *J* = 5.9 Hz, 3H), 1.60–1.76 (m, 3H), 1.92 (tt, *J* = 6.6, 7.2 Hz, 2H), 2.97 (t, *J* = 7.6 Hz, 2H), 3.14 (dt, *J* = 6.2, 6.6 Hz, 2H), 3.55 (dt, *J* = 6.7, 7.0 Hz, 2H), 4.26–4.41 (m, 1H), 4.55 (t, *J* = 7.2 Hz, 2H), 6.86–7.53 (brm, 8H), 6.99 (m, 1H), 7.03–7.11 (m, 2H), 7.20 (br, 1H), 7.33–7.43 (m, 2H), 7.55 (d, *J* = 9.0 Hz, 1H), 7.59 (d, *J* = 7.9 Hz, 1H), 7.73 (t, *J* = 5.4 Hz, 1H), 7.90 (d, *J* = 9.0 Hz, 1H), 7.95–7.99, (br, 1H), 8.65 (t, *J* = 5.7 Hz, 1H), 10.08 (s, 1H), 10.82 (s, 1H); LRMS (FAB): 573 (MH^+, base peak), 444; HRMS (FAB): calcd for $C_{36}H_{41}N_{16}O_2$ (MH^+) 573.3414; found 573.3418. Compound (*S*)-**10h**: $[\alpha]_D^{23}$ 3.3(c0.34, CH_3OH); ^1H NMR (500 MHz, DMSO-d_6): δ = 1.91 (tt, *J* = 7.2, 7.4 Hz, 2H), 2.96 (t, *J* = 7.3 Hz, 2H), 2.97–3.04 (m, 1H), 3.13 (dt, *J* = 5.4, 7.2 Hz, 2H), 3.20–3.27 (m, 1H), 3.54 (dt, *J* = 6.0, 7.3 Hz, 2H), 4.54 (t, *J* = 7.4 Hz, 2H), 4.56–4.62 (m, 1H), 6.78–7.64 (brm, 8H), 6.98 (m, 1H), 7.03–7.10 (m, 2H), 7.19 (m, 1H), 7.21–7.27 (m, 1H), 7.27–7.40 (m, 6H), 7.55 (d, *J* = 8.9 Hz, 1H), 7.58 (d, *J* = 7.7 Hz, 1H), 7.71 (t, *J* = 5.3 Hz, 1H), 7.85 (d, *J* = 8.9 Hz, 1H), 7.89–7.92, (br, 1H), 8.64 (t, *J* = 6.0 Hz, 1H), 10.12 (br, 1H), 10.82 (br, 1H); LRMS (FAB): 607 (MH^+, base peak), 444; HRMS (FAB): calcd for $C_{33}H_{39}N_{16}O_2$ (MH^+) 607.3257; found 607.3251.

14. Tamamura, H.; Hiramatsu, K.; Ueda, S.; Wang, Z.; Kusano, S.; Terakubo, S.; Trent, J. O.; Peiper, S. C.; Yamamoto, N.; Nakashima, H.; Otaka, A.; Fujii, N. *J. Med. Chem.* **2005**, *48*, 380.

Bioorganic & Medicinal Chemistry 16 (2008) 9184–9187

Contents lists available at ScienceDirect

Bioorganic & Medicinal Chemistry

journal homepage: www.elsevier.com/locate/bmc

Identification of minimal sequence for HIV-1 fusion inhibitors

Hiroki Nishikawa [a], Shinya Oishi [a], Mizuno Fujita [a], Kentaro Watanabe [a], Rei Tokiwa [a], Hiroaki Ohno [a], Eiichi Kodama [b], Kazuki Izumi [b], Keiko Kajiwara [b], Takeshi Naitoh [b], Masao Matsuoka [b], Akira Otaka [a,c], Nobutaka Fujii [a,*]

[a] Graduate School of Pharmaceutical Sciences, Kyoto University, Sakyo-ku, Kyoto 606-8501, Japan
[b] Laboratory of Virus Control, Institute for Virus Research, Kyoto University, Sakyo-ku, Kyoto 606-8507, Japan
[c] Graduate School of Pharmaceutical Sciences, The University of Tokushima, Tokushima 770-8505, Japan

ARTICLE INFO

Article history:
Received 7 August 2008
Revised 29 August 2008
Accepted 5 September 2008
Available online 10 September 2008

Keywords:
HIV-1
Fusion inhibitor
α-Helix
Heptad repeat

ABSTRACT

Emergence of multi-drug resistant HIV-1 is a serious problem for AIDS treatment. Recently, the virus-cell membrane fusion process has been identified as a promising target for the development of novel drugs against these resistant variants. In this study, we identified a 29-residue peptide fusion inhibitor, SC29EK, which shows activity comparable to the previously reported inhibitor SC35EK. Some residues in SC29EK not required for interaction with virus gp41 heptad repeat 1 (HR1) were replaced with a non-proteinogenic amino acid, 2-aminoisobutyric acid (Aib), to stabilize the α-helix structure and to provide resistance to peptidases.

1. Introduction

Emergence of HIV-1 variants resistant to clinically approved inhibitors such as reverse transcriptase (RT) or viral protease is a serious problem in AIDS treatment.[1] Therefore, development of novel anti-HIV-1 drugs suppressing such resistant variants is urgently required. In this regard, inhibitors that target other processes, including integration, receptor binding or fusion have been proposed to suppress such resistant variants.[2–6] We and others have recently focused on viral fusion to host cells for development of novel anti-HIV agents that effectively inhibit HIV-1 replication with fewer resistant variants and adverse side effects.[7–9] Among envelope glycoproteins, gp41 in particular plays a pivotal role in the fusion process. Briefly, gp41 in trimer anchors to the host cell membrane, and two extra-virion α-helical regions, designated as heptad repeats 1 and 2 (HR1 and HR2), form an anti-parallel 6-helix bundle by the interaction between HR1 and HR2, leading to fusion of HIV-1 with the cell membrane.[10]

Enfuvirtide (T-20) **1**, which is derived from the gp41 HR2 region, is the only clinically approved peptide fusion inhibitor.[11] Although this agent is effective against variants resistant to multiple RT- and protease-inhibitors as well as wild-type strains,[12,13] T-20-resistant HIV-1 strains have emerged after T-20-containing therapy.[14,15] Thus, the development of second generation fusion inhibitors that suppress T-20-resistant variants is urgently needed. T-20 **1** and another HR2 peptide C34 **2** show the anti-HIV activity by binding with the viral gp41 HR1 to disturb the 6-helix bundle formation (Table 1).[10a] Previously, we developed the novel potent fusion inhibitors T-20EK[16] **3** and SC35EK[9] **4**, which are derived from T-20 **1** and C34 **2**, respectively. On the basis of the α-helical structure of these HR2 peptides upon binding with HR1,[17] we distinguished two surfaces: a virus HR1 interactive site and a solvent-accessible site (Fig. 1). For the residues at the solvent-accessible site (b, c, f, and g in Fig. 1), a series of systematic replacements with hydrophilic glutamic acid (E) or lysine (K) was introduced (EK motif) to enhance the α-helicity of the HR2 peptides by possible intrahelical salt-bridges. On the other hand, the residues at the interactive site (a, d, and e in Fig. 1) were retained for binding affinity. The stabilized bioactive α-helix conformation led to increased anti-HIV-1 activity through higher affinity with the virus HR1 region. 2-Aminoisobutyric acid (Aib), which could enhance and/or stabilize α-helicity of the peptides,[18,19] and may confer peptidase resistance,[20] was also applied to the modification of α-helix inducible EK motifs.

In this study, we investigated the minimal sequence of C34 **2** and SC35EK **4** for potent anti-HIV activity. In addition, modifications of each EK motif with Aib-containing motifs were examined.

2. Results and discussion

We and other groups have reported that C34 **2** and its derivatives interact with N36, a representative peptide of the gp41 HR1

* Corresponding author. Tel.: +81 75 753 4551; fax: +81 75 753 4570.
E-mail address: nfujii@pharm.kyoto-u.ac.jp (N. Fujii).

0968-0896/$ - see front matter © 2008 Elsevier Ltd. All rights reserved.
doi:10.1016/j.bmc.2008.09.018

Table 1
Sequences and anti-HIV activities of C34 and its derivatives, and T_m values of the mixture with N36

Peptide		Sequence	EC_{50} (nM)[a]	T_m (°C)[b]
T-20	**1**	YTSLIHSLIEESQNQQEKNEQELLELDKWASLWNWF	15	ND[c]
C34	**2**	WMEWDREINNYTSLIHSLIEESQNQQEKNEQELL	0.68	52.5
T-20EK	**3**	YTSLIEELIKKSEEQQKKNEEKLKKLEEWAKKWNWF	1.8	N.D.[c]
SC35EK	**4**	WEEWIKKIEEYTKKIEELIKKSEEQQKKNEELKK	0.39	71.5
C29	**5**	WMEWDREINNYTSLIHSLIKESQNQQEEN	46	48.5
C22	**6**	WMEWDREINNYTSLIHSLIKES	>1000	38.5
SC29EK	**7**	WEEWIKKIEEYTKKIEELIKKSEEQQKKN	0.46	65.0
SC22EK	**8**	WEEWIKKIEEYTKKIEELIKKS	60	63.5

[a] EC_{50} was determined as the concentration that blocked HIV-1 replication by 50%.
[b] T_m values were defined by the midpoint of the thermal unfolding transition state (Fig. 4).
[c] ND, not determined.

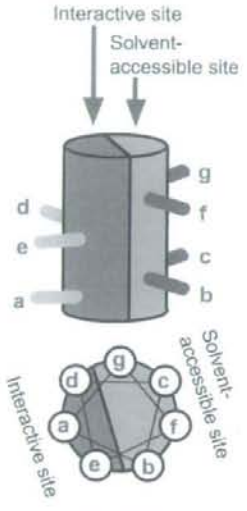

Figure 1. The design concept and helical wheel representation of HIV-1 gp41 HR2 peptide analogues. In the heptad repeat of α-helix, positions a, d, e and positions b, c, f, g represent the viral HR1 interactive and solvent-accessible site, respectively.

region.[9,19,21] In these reports, N-terminal tryptophan rich domain (WRD) containing two tryptophan residues of C34 **2** is essential for the interaction with the HR1 region,[22] while the C-terminal sequence might not be important compared to the N-terminal.[19,23] In order to identify the minimal N-terminal sequence of C34 **2** and SC35EK **4**, we designed two C-terminally truncated peptides C29 **5** and C22 **6** as well as the EK-motif-containing congeners SC29EK **7** and SC22EK **8**, respectively (Table 1). The anti-HIV activity of these peptides was examined by MAGI assay.[24,25] C29 **5** and C22 **6** showed marginal activity compared to the original C34 **2**,[19,26,27] while anti-HIV activity of SC29EK **7** possessing four EK motifs was comparable to that of C34 **2** and SC35EK **4**. Further truncation of an EK motif resulted in a significant decrease in anti-HIV activity (SC22EK **8**; EC_{50} = 60 nM). It is of note that SC29EK **7** and SC22EK **8** with EK motifs showed more potent activity than the original peptides C29 **5** and C22 **6**, respectively.

The potent anti-HIV activity of HR2-derived fusion inhibitors can be rationalized by the facilitated bioactive α-helix conformation, which is favorable for binding with the gp41 HR1 region.[9,28] Wavelength-dependent circular dichroism (CD) spectra of SC29EK **7** at 25 °C showed characteristic spectrum minima at 208 and 222 nm, which indicate the presence of a stable α-helical conformation, as observed in SC35EK **4** (Fig. 2). On the other hand, SC22EK **8** showed slightly less α-helicity compared with SC35EK **4** and SC29EK **7**, indicating that the truncated sequence of **8** may be insufficient to stabilize the α-helix structure. Native peptides, C34 **2**, C29 **5**, and C22 **6** exhibited similar spectra indicating the random structure (Fig. 2).

The binding affinities were estimated by measuring the CD spectra of HR2 peptides **2** and **4–8** in the presence of equimolar amount of N36 (HR1 region peptide). Similar spectra were observed in all N36/C34 derivative complexes except for the N36/C22 **6** complex, indicating that these peptide mixtures contained the similar stable 6-helix conformation at 25 °C (Fig. 3). Less stable coiled-coil structure of the N36/C22 **6** complex was consistent with the deficient anti-HIV activity of C22 **6**. Thermal stabilities of possible 6-helix bundle structures consisting of N36 and C34 derivatives were also evaluated by monitoring the CD signal at 222 nm. Melting temperature (T_m) of the complex was defined as the midpoint of thermal unfolding transition state shown in CD profiles (Fig. 4). T_m values of N36/SC35EK **4**, N36/SC29EK **7**, and N36/SC22EK **8** mixtures were 71.5, 65.0, and 63.5 °C, respectively, which were higher than those of the corresponding mixtures of native sequences [T_m (N36/C34 **2**) = 52.5 °C, T_m (N36/C29 **5**) = 48.5 °C, and T_m (N36/C22 **6**) = 38.5 °C] (Fig. 4). These results indicate that the introduction of EK motifs to HR2 peptides enhances binding affinity with the HR1 region, which could provide more potent anti-HIV activity. It should be noted that SC22EK **8** showed less potent anti-HIV activity compared with the other EK motif-containing peptides, although the thermal stabilities were similar. The limited coverage of the HR1 region by the truncated sequence of **8** may be inadequate for complete inhibition against folding of viral gp41 even with high binding affinity. As such, the potent anti-HIV activity of SC29EK **7** is rationalized by the presence of minimal interactive residues as well as the stabilized bioactive α-helix conformation induced by EK motifs.

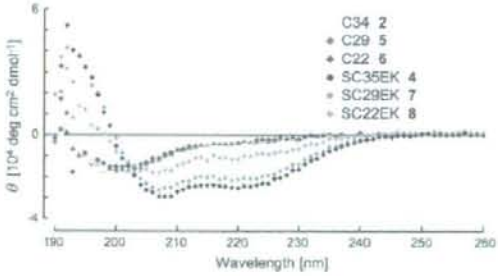

Figure 2. CD spectra of HR2 peptide analogues.

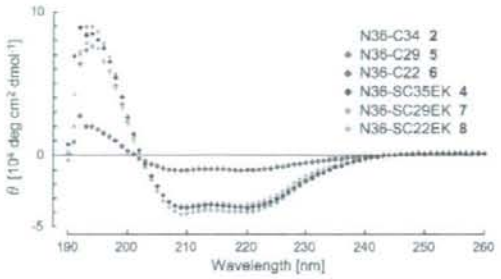

Figure 3. CD spectra of HR2 peptide analogues in the presence of equimolar amount of N36.

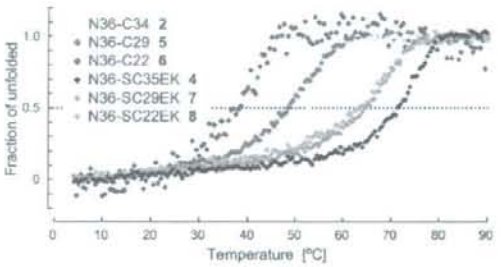

Figure 4. Thermal midpoint analysis of CD signal at 222 nm for HR1 (N36) and HR2 peptide complex.

Since the residues at the solvent-accessible sites of HR2 peptides have no direct involvement in the interaction with the viral HR1 region, we expected that these EK motifs could be replaced with other α-helix-inducible units. Replacement of a part of the EK motifs in SC29EK **7** with a pair of Aib-containing dipeptides such as Aib-Glu (***aE***) and Aib-Lys (***aK***) was attempted (peptides **9–12**, Fig. 5 and Table 2).[18,20] Anti-HIV activities of the Aib-substituted peptides **9–12** were equipotent or lower compared with SC29EK **7**. Peptide **9**, which was modified with a pair of ***aE*** and ***aK*** dipeptides at the essential WRD of the HR2 peptide[22] was the most potent, with the bioactivity almost identical to that of the parent SC29EK **7** (Table 2). This indicated that EK residues could be replaced with non-proteinogenic and α-helix inducible Aib residues, which may also enhance the biostability in vivo. In order to investigate the effect of the remaining Glu-Lys pairing in the ***aE/aK*** motif, we further substituted these residues with glycine (Gly)

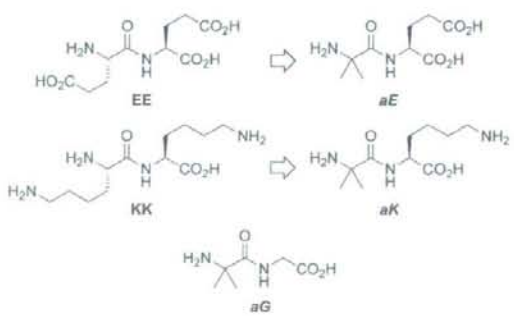

Figure 5. Substitution of an EE or KK unit with Aib-Glu (***aE***), Aib-Lys (***aK***), or Aib-Gly (***aG***).

Table 2
Sequences and anti-HIV activities of SC29EK analogues containing aminoisobutyric acid (Aib) residue

Peptide	Sequence	EC_{50}[a] (nM)
7	WEEWDKKIEEYTKKIEELIKKSEEQQKKN	0.46
9	WaEWDaKIEEYTKKIEELIKKSEEQQKKN	0.54
10	WEEWDKKIaEYTaKIEELIKKSEEQQKKN	2.15
11	WEEWDKKIEEYTKKIaELIaKSEEQQKKN	0.87
12	WEEWDKKIEEYTKKIEELIKKSaEQQaKN	7.10
13	WaGWDaGIEEYTKKIEELIKKSEEQQKKN	37.5
14	WEEWDKKIaGYTaGIEELIKKSEEQQKKN	270
15	WEEWDKKIEEYTKKIaGLIaGSEEQQKKN	25.6
16	WEEWDKKIEEYTKKIEELIKKSaGQQaGN	31.3

[a] EC_{50} was determined as the concentration that blocked HIV-1 replication by 50%.

(peptides **13–16**) (Fig. 5 and Table 2). All substituted peptides **13–16** showed significantly less potent anti-HIV activity compared with the corresponding peptides **9–12** containing an ***aE/aK*** motif (Table 2), suggesting that modification of an EK motif with two Aib-Gly (***aG***) is not suitable for potent anti-HIV activity.

3. Conclusions

In this study, we identified the minimal bioactive sequence of HIV-1 fusion inhibitors and developed a novel potent fusion inhibitory peptide SC29EK **7** based on the previously reported SC35EK **4**. SC29EK **7** reproduced potent anti-HIV-1 activity comparable to SC35EK **4**. The introduction of α-helix-inducible EK motifs to less potent C29 **5** recovered the bioactivity of the parent C34 **2**, indicating that binding of the C29 sequence containing essential tryptophan rich domain to the gp41 HR1 is sufficient for anti-HIV activity. Moreover, it was also demonstrated that some EK motifs are replaceable with other non-proteinogenic amino acids such as 2-aminoisobutyric acid (Aib). These results may lead to development of more potent HIV-1 fusion inhibitors.

4. Experimental

4.1. Peptide synthesis

Protected peptide-resins were manually constructed by Fmoc-based solid-phase peptide synthesis. *t*-Bu ester for Asp and Glu; 2,2,4,6,7-pentamethyldihydrobenzofuran-5-sulfonyl (Pbf) for Arg; *t*-Bu for Thr; Tyr and Ser; Boc for Lys; and Trt for Gln, Asn, and His were employed for side-chain protection. Fmoc-amino acids were coupled using five equivalents of reagents [Fmoc-amino acid, *N,N'*-diisopropylcarbodiimide (DIPCDI), and HOBt·H_2O] in DMF for 1.5 h. Fmoc deprotection was performed with 20% piperidine in DMF (2 × 1 min, 1 × 20 min). The resulting protected resin was treated with TFA/thioanisole/*m*-cresol/1,2-ethandithiol/H_2O (80:5:5:5:5) at room temperature for 2 h. After removal of the resin by filtration, the filtrate was poured into ice-cold dry diethyl ether. The resulting powder was collected by centrifugation and washed with ice-cold dry diethyl ether. The crude product was purified by preparative HPLC on a Cosmosil 5C18-ARII preparative column (Nacalai Tesque, 20 × 250 mm, flow rate 10 mL/min) to afford the expected peptides. All peptides were characterized by an ESI-MS (Sciex API*III*E, Toronto, Canada) or MALDI-TOF-MS (AXIMA-CFR plus, Shimadzu, Kyoto, Japan), and the purity was calculated as >95% by HPLC on a Cosmosil 5C18-ARII analytical column (Nacalai Tesque, 4.6 × 250 mm, flow rate 1 mL/min) at 220 nm absorbance. The detailed MS data are shown in Table 3.

Table 3
Mass spectrum data of synthesized peptides

Peptide	Calculated MW ($M+H^+$)		Observed MW
1	$C_{204}H_{302}N_{51}O_{64}$	4492.9	4492.5[a]
2	$C_{186}H_{284}N_{51}O_{64}S$	4290.6	4289.3[a]
3	$C_{213}H_{329}N_{52}O_{62}$	4626.2	4625.5[a]
4	$C_{203}H_{326}N_{51}O_{66}$	4537.1	4536.3[a]
5	$C_{159}H_{240}N_{45}O_{54}S$	3677.9	3677.7[a]
6	$C_{125}H_{185}N_{32}O_{46}S$	2808.1	2808.1[a]
7	$C_{170}H_{270}N_{43}O_{54}$	3780.2	3779.5[a]
8	$C_{134}H_{210}N_{31}O_{40}$	2895.3	2895.2[a]
9	$C_{167}H_{265}N_{42}O_{52}$	3693.1	3693.5[b]
10	$C_{167}H_{265}N_{42}O_{52}$	3693.1	3693.5[b]
11	$C_{167}H_{265}N_{42}O_{52}$	3693.1	3692.5[b]
12	$C_{167}H_{265}N_{42}O_{52}$	3693.1	3693.8[b]
13	$C_{160}H_{252}N_{41}O_{50}$	3550.0	3550.1[b]
14	$C_{160}H_{252}N_{41}O_{50}$	3550.0	3549.5[b]
15	$C_{160}H_{252}N_{41}O_{50}$	3550.0	3550.2[b]
16	$C_{160}H_{252}N_{41}O_{50}$	3550.0	3550.2[b]

[a] MALDI-TOF-MS.
[b] ESI-MS (reconstructed).

4.2. Viruses and cells

An infectious clone pNL4-3 (GenBank Accession No. AF324493) was used for the construction and production of HIV-1 as described previously.[29] A wild-type HIV-1 was generated by transfection of pNL4-3 into 293T cells. HeLa-CD4-LTR-β-gal cells (MAGI cells) were kindly provided by Dr. Emerman through the AIDS Research and Reference Reagent Program, Division of AIDS, National Institute of Allergy and Infectious Disease (NIAID) (Bethesda, MD, USA).

4.3. Anti-HIV-1 activity

Anti-HIV-1 activity was determined by the multinuclear activation of a galactosidase indicator (MAGI) assay as described previously.[24,25] Briefly, the MAGI cells (10^4 cells/well) were seeded in flat bottomed 96-well microtitre plates. The following day, the cells were inoculated with HIV-1 (60 MAGI units/well, yielding 60 blue cells after 48 h incubation) and cultured in the presence of various concentrations of peptide inhibitors in fresh medium. After 48 h incubation, all the blue cells stained with 5-bromo-4-chloro-3-indolyl-β-D-galactopyranoside (X-gal) in each well were counted. The activity of inhibitors was determined as the concentration that blocked HIV-1 replication by 50% (50% effective concentration [EC_{50}]).

4.4. CD measurement

An HR2 peptide (peptides **2** and **4–8**) was dissolved in PBS pH 7.4 at a concentration of 10 μM. At the CD measurement of mixture of an HR1 peptide (N36) and an HR2 peptide or its analogues, the peptides were incubated at 37 °C for 30 min (final concentration of both HR1 peptide and HR2 peptide was 10 μM in PBS, pH 7.4). The wavelength-dependent of molar ellipticity [θ] was monitored at 25 °C as the average of eight scans, and the thermal stability of the HR1 and HR2 mixture was estimated by monitoring the change in the CD signal at 222 nm in a spectropolarimeter (Model J-710; Jasco, Tokyo, Japan) equipped with a thermoelectric temperature controller. The midpoint of thermal unfolding transition (melting temperature [T_m]) of each complex was determined as described previously.[9]

Acknowledgments

This work was supported in part by grants for the Promotion of AIDS Research from the Ministry of Health and Welfare and the Ministry of Education, Culture, Sports, Science, and Technology of Japan (E.K. and S.O.); a grant for Research for Health Sciences Focusing on Drug Innovation from The Japan Health Sciences Foundation (E.K., S.O., N.F., and M.M.); and the 21st Century COE program "Knowledge Information Infrastructure for Genome Science" (N.F. and H.N.). H.N. is grateful for the JSPS Research Fellowships for Young Scientists. Appreciation is expressed to Mr. Maxwell Reback (Kyoto University) for reading the manuscript.

References and notes

1. Clavel, F.; Hance, A. J. *N. Engl. J. Med.* **2004**, *350*, 1023.
2. Fatkenheuer, G.; Pozniak, A. L.; Johnson, M. A.; Plettenberg, A.; Staszewski, S.; Hoepelman, A. I.; Saag, M. S.; Goebel, F. D.; Rockstroh, J. K.; Dezube, B. J.; Jenkins, T. M.; Medhurst, C.; Sullivan, J. F.; Ridgway, C.; Abel, S.; James, I. T.; Youle, M.; van der Ryst, E. *Nat. Med.* **2005**, *11*, 1170.
3. Grinsztejn, B.; Nguyen, B. Y.; Katlama, C.; Gatell, J. M.; Lazzarin, A.; Vittecoq, D.; Gonzalez, C. J.; Chen, J.; Harvey, C. M.; Isaacs, R. D. *Lancet* **2007**, *369*, 1261.
4. Hazuda, D. J.; Young, S. D.; Guare, J. P.; Anthony, N. J.; Gomez, R. P.; Wai, J. S.; Vacca, J. P.; Handt, L.; Motzel, S. L.; Klein, H. J.; Dornadula, G.; Danovich, R. M.; Witmer, M. V.; Wilson, K. A.; Tussey, L.; Schleif, W. A.; Gabryelski, L. S.; Jin, L.; Miller, M. D.; Casimiro, D. R.; Emini, E. A.; Shiver, J. W. *Science* **2004**, *305*, 528.
5. Root, M. J.; Kay, M. S.; Kim, P. S. *Science* **2001**, *291*, 884.
6. Tagat, J. R.; McCombie, S. W.; Nazareno, D.; Labroli, M. A.; Xiao, Y.; Steensma, R. W.; Strizki, J. M.; Baroudy, B. M.; Cox, K.; Lachowicz, J.; Varty, G.; Watkins, R. *J. Med. Chem.* **2004**, *47*, 2405.
7. Bewley, C. A.; Louis, J. M.; Ghirlando, R.; Clore, G. M. *J. Biol. Chem.* **2002**, *277*, 14238.
8. Dwyer, J. J.; Wilson, K. L.; Davison, D. K.; Freel, S. A.; Seedorff, J. E.; Wring, S. A.; Tvermoes, N. A.; Matthews, T. J.; Greenberg, M. L.; Delmedico, M. K. *Proc. Natl. Acad. Sci. U.S.A.* **2007**, *104*, 12772.
9. Otaka, A.; Nakamura, M.; Nameki, D.; Kodama, E.; Uchiyama, S.; Nakamura, S.; Nakano, H.; Tamamura, H.; Kobayashi, Y.; Matsuoka, M.; Fujii, N. *Angew. Chem. Int. Ed. Engl.* **2002**, *41*, 2937.
10. (a) Chan, D. C.; Kim, P. S. *Cell* **1998**, *93*, 681; (b) Eckert, D. M.; Kim, P. S. *Annu. Rev. Biochem.* **2001**, *70*, 777.
11. Matthews, T.; Salgo, M.; Greenberg, M.; Chung, J.; DeMasi, R.; Bolognesi, D. *Nat. Rev. Drug Discov.* **2004**, *3*, 215.
12. Lalezari, J. P.; Henry, K.; O'Hearn, M.; Montaner, J. S.; Piliero, P. J.; Trottier, B.; Walmsley, S.; Cohen, C.; Kuritzkes, D. R.; Eron, J. J., Jr.; Chung, J.; DeMasi, R.; Donatacci, L.; Drobnes, C.; Delehanty, J.; Salgo, M. *N. Engl. J. Med.* **2003**, *348*, 2175.
13. Lazzarin, A.; Clotet, B.; Cooper, D.; Reynes, J.; Arasteh, K.; Nelson, M.; Katlama, C.; Stellbrink, H. J.; Delfraissy, J. F.; Lange, J.; Huson, L.; DeMasi, R.; Wat, C.; Delehanty, J.; Drobnes, C.; Salgo, M. *N. Engl. J. Med.* **2003**, *348*, 2186.
14. Poveda, E.; Rodes, B.; Toro, C.; Martin-Carbonero, L.; Gonzalez-Lahoz, J.; Soriano, V. *AIDS* **2002**, *16*, 1959.
15. Wei, X.; Decker, J. M.; Liu, H.; Zhang, Z.; Arani, R. B.; Kilby, J. M.; Saag, M. S.; Wu, X.; Shaw, G. M.; Kappes, J. C. *Antimicrob. Agents Chemother.* **2002**, *46*, 1896.
16. Oishi, S.; Ito, S.; Nishikawa, H.; Watanabe, K.; Tanaka, M.; Ohno, H.; Izumi, K.; Sakagami, Y.; Kodama, E.; Matsuoka, M.; Fujii, N. *J. Med. Chem.* **2008**, *51*, 388.
17. Chan, D. C.; Fass, D.; Berger, J. M.; Kim, P. S. *Cell* **1997**, *89*, 263.
18. Karle, I. L.; Balaram, P. *Biochemistry* **1990**, *29*, 6747.
19. Sia, S. K.; Carr, P. A.; Cochran, A. G.; Malashkevich, V. N.; Kim, P. S. *Proc. Natl. Acad. Sci. U.S.A.* **2002**, *99*, 14664.
20. Yamaguchi, H.; Kodama, H.; Osada, S.; Kato, F.; Jelokhani-Niaraki, M.; Kondo, M. *Biosci. Biotechnol. Biochem.* **2003**, *67*, 2269.
21. Liu, S.; Lu, H.; Niu, J.; Xu, Y.; Wu, S.; Jiang, S. *J. Biol. Chem.* **2005**, *280*, 11259.
22. Chan, D. C.; Chutkowski, C. T.; Kim, P. S. *Proc. Natl. Acad. Sci. U.S.A.* **1998**, *95*, 15613.
23. Gochin, M.; Savage, R.; Hinckley, S.; Cai, L. *Biol. Chem.* **2006**, *387*, 477.
24. Kimpton, J.; Emerman, M. *J. Virol.* **1992**, *66*, 2232.
25. Kodama, E. I.; Kohgo, S.; Kitano, K.; Machida, H.; Gatanaga, H.; Shigeta, S.; Matsuoka, M.; Ohrui, H.; Mitsuya, H. *Antimicrob. Agents Chemother.* **2001**, *45*, 1539.
26. Ji, H.; Shu, W.; Burling, F. T.; Jiang, S.; Lu, M. *J. Virol.* **1999**, *73*, 8578.
27. Shu, W.; Liu, J.; Ji, H.; Radigen, L.; Jiang, S.; Lu, M. *Biochemistry* **2000**, *39*, 1634.
28. Judice, J. K.; Tom, J. Y.; Huang, W.; Wrin, T.; Vennari, J.; Petropoulos, C. J.; McDowell, R. S. *Proc. Natl. Acad. Sci. U.S.A.* **1997**, *94*, 13426.
29. Nameki, D.; Kodama, E.; Ikeuchi, M.; Mabuchi, N.; Otaka, A.; Tamamura, H.; Ohno, M.; Fujii, N.; Matsuoka, M. *J. Virol.* **2005**, *79*, 764.

The International Journal of Biochemistry & Cell Biology 40 (2008) 2410–2420

Contents lists available at ScienceDirect

The International Journal of Biochemistry & Cell Biology

journal homepage: www.elsevier.com/locate/biocel

2′-Deoxy-4′-C-ethynyl-2-halo-adenosines active against drug-resistant human immunodeficiency virus type 1 variants

Atsushi Kawamoto[a], Eiichi Kodama[a,*], Stefan G. Sarafianos[b], Yasuko Sakagami[a], Satoru Kohgo[c], Kenji Kitano[c], Noriyuki Ashida[c], Yuko Iwai[c], Hiroyuki Hayakawa[c], Hirotomo Nakata[d,e], Hiroaki Mitsuya[d,e], Eddy Arnold[f], Masao Matsuoka[a]

[a] Laboratory of Virus Immunology, Institute for Virus Research, Kyoto University, 53 Kawaramachi, Shogoin, Sakyo-ku, Kyoto 606-8507, Japan
[b] Department of Molecular Microbiology and Immunology, University of Missouri-Columbia, School of Medicine and Christopher S. Bond Life Sciences Center, Columbia, MO 65211, USA
[c] Biochemicals Division, Yamasa Corporation, Chiba 288-0056, Japan
[d] Department of Hematology and Infectious Diseases, Kumamoto University School of Medicine, Kumamoto 860-8556, Japan
[e] Experimental Retrovirology Section, HIV and AIDS Malignancy Branch, National Cancer Institute, Bethesda, MD 20892, USA
[f] Center for Advanced Biotechnology and Medicine and Department of Chemistry and Chemical Biology, Rutgers University, Piscataway, NJ 08854, USA

ARTICLE INFO

Article history:
Received 3 December 2007
Received in revised form 14 March 2008
Accepted 2 April 2008
Available online 11 April 2008

Keywords:
Human immunodeficiency virus
Reverse transcriptase inhibitor
Resistance

ABSTRACT

One of the formidable challenges in therapy of infections by human immunodeficiency virus (HIV) is the emergence of drug-resistant variants that attenuate the efficacy of highly active antiretroviral therapy (HAART). We have recently introduced 4′-ethynyl-nucleoside analogs as nucleoside reverse transcriptase inhibitors (NRTIs) that could be developed as therapeutics for treatment of HIV infections. In this study, we present 2′-deoxy-4′-C-ethynyl-2-fluoroadenosine (EFdA), a second generation 4′-ethynyl inhibitor that exerted highly potent activity against wild-type HIV-1 ($EC_{50} \sim 0.07$ nM). EFdA retains potency toward many HIV-1 resistant strains, including the multi-drug resistant clone HIV-$1_{A62V/V75I/F77L/F116Y/Q151M}$. The selectivity index of EFdA (cytotoxicity/inhibitory activity) is more favorable than all approved NRTIs used in HIV therapy. Furthermore, EFdA efficiently inhibited clinical isolates from patients heavily treated with multiple anti-HIV-1 drugs. EFdA appears to be primarily phosphorylated by the cellular 2′-deoxycytidine kinase (dCK) because: (a) the antiviral activity of EFdA was reduced by the addition of dC, which competes nucleosides phosphorylated by the dCK pathway, (b) the antiviral activity of EFdA was significantly reduced in dCK-deficient HT-1080/Ara-C^r cells, but restored after dCK transduction. Further, unlike other dA analogs, EFdA is completely resistant to degradation by adenosine deaminase. Moderate decrease in susceptibility to EFdA is conferred by a combination of three RT mutations (I142V, T165R, and M184V) that result in a significant decrease of viral fitness. Molecular modeling analysis suggests that the M184V/I substitutions may reduce anti-HIV activity of EFdA through steric hindrance between its 4′-ethynyl moiety and the V/I184 β-branched side chains. The present data suggest that EFdA, is a promising candidate for developing as a therapeutic agent for the treatment of individuals harboring multi-drug resistant HIV variants.

1. Introduction

Highly active antiretroviral therapies (HAART), combining two or more reverse transcriptase inhibitors (RTIs) and/or protease inhibitors, have been successful in sig-

* Corresponding author. Tel.: +81 75 751 3986; fax: +81 75 751 3986.
E-mail address: ekodama@virus.kyoto-u.ac.jp (E. Kodama).

1357-2725/$ – see front matter © 2008 Elsevier Ltd. All rights reserved.
doi:10.1016/j.biocel.2008.04.007

nificantly reducing viral loads and bringing about clinical benefits to the treatment of patients infected with human immunodeficiency virus type 1 (HIV-1). Although HAART improves prognosis for HIV-1 infected patients (Palella et al., 1998), drug-resistant viruses emerge during prolonged therapy and some resistant viruses show intra-class cross resistance. Moreover, drug-resistant variants can be transmitted to other individuals as primary infections (Little et al., 2002). Hence, there is a great need for the development of new HIV inhibitors that retain activity against drug-resistant HIV variants.

In this regard, we have focused on the family of nucleoside reverse transcriptase inhibitors (NRTIs) and have previously reported that a series of 2′-deoxy-4′-*C*-ethynyl-nucleosides (EdNs) efficiently suppress (EC_{50}s as low as one nanomolar) various NRTI-resistant HIV strains including multi-drug resistant clinical isolates (Kodama et al., 2001). More recently, Haraguchi and others have reported that additional members of EdNs such as 2′,3′-didehydro-3′-deoxy-4′-*C*-ethynyl-thymidine (Ed4T) are also active against wild-type and drug-resistant strains (EC_{50}s ranged from 0.16 to 17 μM) and less toxic than d4T (also known as stavudine) *in vitro* (Dutschman et al., 2004; Haraguchi et al., 2003), while 4′-Ed4T is only moderately active against (−)-2′,3′-dideoxy-3′-thiacytidine (3TC or lamivudine)-resistant HIV-1_{M184V} (Nitanda et al., 2005).

To further increase the antiviral activity and reduce the cytotoxicity, we designed and synthesized a second generation of 4′-substituted adenosine analogs with halogen substitutions at their 2-position. We report here that 2′-deoxy-4′-*C*-ethynyl-2-fluoroadenosine (EFdA) exhibits the highest antiviral activity than any other NRTI when assayed against wild-type or NRTI-resistant HIV clones and clinical isolates from patients treated extensively with anti-HIV agents. In addition, unlike other adenosine-based NRTIs, EFdA showed adenosine deaminase (ADA) resistance. We also show that EFdA is primarily activated through phosphorylation by cellular deoxycytidine kinase (dCK). Molecular modeling analysis has been used to rationalize the resistance profile of these analogs toward key NRTI mutations.

2. Materials and methods

2.1. Compounds

3′-Azido-3′-deoxythymidine (AZT, or zidovudine), 2′,3′-dideoxyinosine (ddI, or didanosine), and 2′,3′-dideoxycytidine (ddC, or zalcitabine) were purchased from Sigma (St. Louis, MO.). 3TC was kindly provided from S. Shigeta (Fukushima Medical University, Fukushima, Japan). A set of EdN analogs were designed and synthesized as described elsewhere (Ohrui, 2006). Their chemical structures are shown in Fig. 1. 2′-Deoxycoformycin (dCF) was synthesized in Yamasa Corporation (Choshi, Japan).

2.2. Cells and plasmids

MT-2 and MT-4 cells were grown in an RPMI 1640-based culture medium, and 293T cells were grown in Dulbecco's modified Eagle medium (DMEM); each of these media was

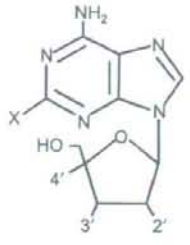

Base X	Sugar 2′	Sugar 3′	4′	Compound abbreviation
-H	-H	-OH	-C ≡ CH	*E*dA
-F	-H	-OH	-C ≡ CH	2F-*E*dA
-F	-H	-H	-C ≡ CH	2F-*E*ddA
-F	C = C		-C ≡ CH	2F-*E*d4A
-F	-H	-OH	-C ≡ N	2F-CNdA
-Cl	-H	-OH	-C ≡ CH	2Cl-*E*dA

Fig. 1. Structures of 4′-substituted adenosine analogs. All nucleoside analogs discussed here have substitutions at the 4′-position of the sugar ring.

supplemented with 10% fetal calf serum (FCS), 2 mM L-glutamine, 100 U/ml penicillin, and 50 μg/ml streptomycin. HeLa-CD4-LTR/β-galactosidase (MAGI) cells were propagated in DMEM supplemented with 10% FCS, 0.2 mg/ml of hygromycin B, and 0.2 mg/ml of G418 (Kimpton and Emerman, 1992). HeLa-CD4/CCR5-LTR/β-galactosidase cells were propagated in puromycin (10 μg/ml) containing DMEM with hygromycin and G418. Peripheral blood mononuclear cells (PBMCs) were obtained from healthy HIV-1-seronegative donors by Ficoll-Hypaque gradient centrifugation and stimulated for 3 days with phytohemagglutinin M (PHA; 10 μg/ml; Sigma) and recombinant human interleukin 2 (IL-2; 10 U/ml; Shionogi & Co., Ltd., Osaka, Japan) prior to use. Human fibrosarcoma cell lines, HT-1080 and HT-1080/Ara-C^r were grown in the RPMI-based culture medium (Obata et al., 2001). To express HIV-1 receptors, we constructed a mammalian expression vector pBC-CD4/CXCR4-IH, which encodes CD4, CXCR4, and hygromycin phosphotransferase with two internal ribosome entry sites under control of cytomegalovirus promoter as described (Kajiwara et al., 2006). After the transfection into HT-1080 and HT-1080/Ara-C^r, cells were selected by 0.2 mg/ml hygromycin B. For the expression of human deoxycytidine kinase (dCK), pCI-neo (Promega, Madison, WI)-based plasmid, pCI-dCK, was transfected into HT-1080/Ara-C^r and selected with 0.2 mg/ml G418. Established cells were designated HT-1080/Ara-C^r/dCK. Puromycin resistance gene under the control of PGK promoter was inserted into pLTR-SEAP (Miyake et al., 2003), which encodes a secreted form of the placental alkaline phosphatase (SEAP) gene under control of the HIV-1 long terminal repeat (LTR) (pLTR-SEAP-$puro^r$). pLTR-SEAP-$puro^r$ was transfected into the three HT-1080 cell lines and selected with 10 μg/ml puromycin.